



**Calhoun: The NPS Institutional Archive**  
**DSpace Repository**

---

Theses and Dissertations

1. Thesis and Dissertation Collection, all items

---

1949

## Noise and noise figure in microwave receivers

Murphy, Thomas Watson

Annapolis, Maryland. U.S. Naval Postgraduate School

---

<http://hdl.handle.net/10945/31642>

---

This publication is a work of the U.S. Government as defined in Title 17, United States Code, Section 101. Copyright protection is not available for this work in the United States.

*Downloaded from NPS Archive: Calhoun*



Calhoun is the Naval Postgraduate School's public access digital repository for research materials and institutional publications created by the NPS community. Calhoun is named for Professor of Mathematics Guy K. Calhoun, NPS's first appointed -- and published -- scholarly author.

**Dudley Knox Library / Naval Postgraduate School**  
**411 Dyer Road / 1 University Circle**  
**Monterey, California USA 93943**

<http://www.nps.edu/library>

NOISE AND NOISE FIGURE IN  
MICROWAVE RECEIVERS

-

T. W. Murphy

Library  
U. S. Naval Postgraduate School  
Annapolis, Md.

NOISE AND NOISE FIGURE IN  
MICROWAVE RECEIVERS

by


Thomas Watson Murphy,  
Lieutenant Commander, United States Navy

Submitted in partial fulfillment  
of the requirements  
for the degree of  
MASTER OF SCIENCE  
in  
ENGINEERING ELECTRONICS

United States Naval Postgraduate School  
Annapolis, Maryland  
1949


This work is accepted as fulfilling  
the thesis requirements for the degree of  
MASTER OF SCIENCE  
in  
ENGINEERING ELECTRONICS

from the  
United States Naval Postgraduate School

  
Chairman

Department of Electronics and Physics

Approved:

  
Academic Dean

11013

## PREFACE

The investigation of noise and noise figure in microwave receivers was commenced in the fall of 1948 at the U. S. Naval Postgraduate School and was continued through the winter in the electronics laboratory of the Glenn L. Martin Company at Middle River, Maryland. This field work was done to give the writer experience in the measurement of noise figure and to acquaint him with the factors contributing to noise in amplifiers as well as the design considerations in the development of a low-noise amplifier.

The writer wishes to express his appreciation for general guidance to Assistant Professor Earl G. Goddard of the U. S. Naval Postgraduate School, and for assistance in the development of techniques for the measurement of noise figure and the design considerations of a low-noise amplifier to Carl S. Chambre' and Howard Weinberger of the Glenn L. Martin Company.

# TABLE OF CONTENTS

	Page
CERTIFICATE OF APPROVAL	i
PREFACE	ii
LIST OF ILLUSTRATIONS	v
TABLE OF SYMBOLS AND ABBREVIATIONS	vi
CHAPTER	
I.    INTRODUCTION	1
II.   NOISE FIGURE	4
1.  Definition and application	4
2.  Available power	4
3.  Available noise power	5
4.  Available output power	5
5.  Available gain	6
6.  Nature of impedances considered	7
7.  Available gain of a few typical networks	7
8.  Noise figures of a few typical networks	10
9.  Consideration of equivalent noise resistance	13
10. Consideration of the partition of the available output noise power	17
11. Effect on noise figure of a temperature difference between antenna and other networks of the receiver	18
12. Noise figure of various amplifier configurations	19
III.  CONTRIBUTIONS TO NOISE IN MICROWAVE RECEIVERS	21
1.  General	21
2.  Antenna noise	22
3.  Crystal converter and local-oscillator noise	24
4.  Thermal agitation noise of input resistance	29
5.  Shot effect and flicker effect	31
IV.   REDUCTION OF NOISE IN RECEIVERS	35
1.  Noise external to the i-f amplifier	35
2.  Internal i-f amplifier noise	38
3.  Consideration of a low-noise amplifier	41
4.  Practical circuit of low-noise amplifier	51
5.  Neutralization considerations	57

## TABLE OF CONTENTS(cont'd)

V.	MEASUREMENT OF NOISE FIGURE	62
	1. Method of measuring noise figure	62
	2. Design of a noise generator	67

BIBLIOGRAPHY	72
--------------	----

## LIST OF ILLUSTRATIONS

	Page
1. Local-oscillator noise as a function of frequency.	28
2. Simple balanced mixer with push-pull i-f transformer to unbalanced line.	37
3. A.c. diagram of cascode low-noise amplifier	41
4. Constant-current equivalent circuit for noise-figure analysis	43
5. Measured excess noise figures of low-noise cascode amplifiers at 6, 30, and 180 Mc.	47
6. Practical embodiment of the low noise cascode in a 30 Mc. i-f preamplifier.	52
7. Design data for low-Q transitionally coupled double-tuned circuit	55
8. Coil neutralization of grid to plate capacitance	58
9. Neutrodyne (Hazeltine) neutralization of grid to plate capacitance.	59
10. Low noise cascode employing a single 2C51 tube in a 30 Mc. i-f preamplifier.	61
11. Schematic of typical noise generator circuit.	63
12. Block diagram of layout used in noise figure measurement.	66
13. Noise generator switching circuit.	69
14. Noise generator control panel.	71



# TABLE OF SYMBOLS AND ABBREVIATIONS

A	open circuit voltage gain
B	bandwidth in cycles per second
$\overline{E}_n^2$	mean-squared noise voltage available from signal generator
e	charge of an electron, $1.6 \times 10^{-19}$ coulomb
F	noise figure
$f_0$	midband frequency
$f_1$	primary frequency of double-tuned circuit
$f_1'$	primary frequency with secondary short-circuited
$f_2$	secondary frequency of double-tuned circuit
$f_2'$	secondary frequency with primary short-circuited
G	available gain
k	Boltzmann's constant - $1.37 \times 10^{-23}$ joules per degree centigrade
K	coefficient of coupling
N	available output noise power
$R_{eq}$	equivalent noise resistance of a vacuum tube
$R_a$	source resistance of signal source
$R_g$	input resistance due to tube and coupling circuits
$R_o$	output impedance of amplifier stage
$R_s$	transformed source resistance of signal source
T	absolute temperature in degrees Kelvin

## CHAPTER I

### INTRODUCTION

In the hope of presenting an easily understandable survey of noise in microwave receivers, the writer has considered the subject from a qualitative point of view without the help of quantum mechanics or a rigorous mathematical analysis of the various phenomena. For one who is interested in exploring the subject more completely, there is a wealth of material available in the literature.

The concept of noise figure has become an increasingly useful tool of the engineer who is interested in the performance to be expected from a radar receiver. Since it appears so frequently in the literature on noise and in the body of this paper, it is presented first as an aid to the understanding of subsequent work.

The next subject in the sequence is that of the various sources contributing to noise in microwave receivers. These noise sources are many and take many forms but in the end they all reduce to two basic concepts, either shot effect or thermal agitation noise.

The first available information on current fluctuation noise in amplifiers is by Schottky (18), in which he predicts the effects to be expected in vacuum tube circuits from probability fluctuations in thermionic emission. These fluctuations, which may best be pictured as shock-excitation of the circuit by the impacts of individual electrons, were designated by Schottky as "shot effect".

The first material on thermal agitation noise in conductors is contained in two short notes by Johnson (7) (8) in which he brought to light the fact that ordinary electric conductors are sources of random voltage fluctuations as the result of thermal agitation of the electric charges in the conductor. To him must go the credit for the universally accepted theory of thermal agitation noise.

Throughout the literature on the subject of noise in amplifiers we are constantly reminded that at one time it seemed that the only sources of noise which could not be eliminated were those external to the circuit. It was felt in earlier days that other sources of noise of purely local origin, such as poor batteries, loose contacts, gassy tubes, and induction from power lines, might be eliminated entirely so that the circuits would be capable of amplifying any signal, no matter how small. It was found, however, that the noise level cannot be lowered indefinitely; that there are limits below which, in the nature of things, noise cannot be reduced.

Of the internal sources of noise, the most fundamental and inevitable is that due to thermal agitation of electrons. In a perfect amplifier, all other noises would be reduced to zero. Next in order comes the influence of ions and shot effect on the current in the vacuum tubes. Under control to a greater extent are the effects of poor contacts and mechanical vibration. In dealing with any of

these disturbances, the circuit and vacuum tube of the first stage of the amplifier are most important, for here the signal is being amplified at its lowest level. When the signal is so faint that it is masked by the noise remaining as the natural limit of the circuit, then the only possible remedy is to raise the signal level.

The natural noise level is exceedingly low, yet modern amplifiers have reached such a stage of perfection that their noise levels often are practically at the natural limit. This is true not only of amplifiers built for experimental purposes, but of many amplifiers used in radio and radar circuits. The natural limits to amplification which will be discussed are, therefore, of very practical interest.

Next for consideration is the subject of reduction of noise in receivers, with emphasis on the design of a low-noise amplifier. There is little doubt that the "cascode" arrangement due to Wallman (21) is the best solution thus far presented and considerable space is devoted to a discussion of this circuit.

Finally, the writer presents his own experience in the measurement of noise figure and in the design of a noise generator for use in such measurement. In this work he has drawn heavily on the experience of others and has introduced refinements from time to time as the need for them become evident.

## CHAPTER II

### NOISE FIGURE

#### 1. Definition and application

The noise figure  $F$  of a network is defined by Friis (4) as the ratio of the "input available signal to available noise power ratio" to the "output available signal to available noise power ratio". Since the term noise figure appears in most of the recent articles on noise, it is introduced prior to the consideration of noise sources. The material here presented is drawn from Friis (4) and Goldberg (5). Several basic concepts are necessary to this discussion and are introduced in the sections following.

#### 2. Available power

The first concept to be considered is that of "available power". A generator of real internal impedance  $R$  ohms and open circuit voltage  $E$  can deliver a maximum power of  $E^2/4R$  watts into a resistive load. This maximum power is delivered only when the generator is matched; i.e. when the load resistor is also  $R$  ohms. Friis terms this maximum power the available power and his designation has been followed in later papers on the subject. This is to most readers an entirely new concept of available power and must be recalled frequently in any treatment of noise figure. It is not to be confused with the power actually available across the terminals of the load resistor unless, of course, that resistor has the same value as the internal resistance of the generator. It is, however, a useful concept in the further treatment of noise figure. Since the available

power is defined as the maximum power the generator can deliver,  $E^2/4R$ , it is independent of the load and dependent only on the characteristics of the generator.

### 3. Available noise power

The definition of available power leads to a concept of "available noise power". It is well known that a resistance of  $R$  ohms at an absolute temperature  $T$  produces a noise voltage across its terminals. This resistance may be represented as a generator having an internal noise-free resistance of  $R$  ohms and an open circuit root-mean-square voltage equal to the square root of  $4kTRB$ . The "available power" from such a generator is by definition  $4kTRB/4R = kTB$ , where  $B$  is the small frequency band over which the noise voltage is measured.

### 4. Available output power

The maximum output power of a network to which a signal generator is connected is termed the "available output power". This maximum power is delivered only when the impedance of the load matches the output impedance of the network. Here, as in the case of the "available power" discussed in Section 2, the available output power is independent of the load on the network. It is not, however, independent of the way in which the signal generator is coupled to the input of the network since the match or mismatch of the input impedance to the internal impedance of the generator will determine how much power is delivered to and by the network.

## 5. Available gain

Gain in this chapter on noise figure refers to power gain and the ratio of "available output power" from the network to the "available signal power" from the generator is termed the "available gain". As pointed out in the preceding sections, it is independent of the load but, since it is a function of the available output power and the available signal power, it is dependent upon the characteristics of the signal generator and the way in which the signal generator is coupled to the network. Goldberg (5) emphasizes this point in saying

The available gain of a network, therefore, is a function of the signal generator used to supply it, and is not a unique characteristic of the network.

Now consider the "available gain" of a cascade of networks. Let us imagine a cascade of networks fed by a signal generator. Measure the available gain of the first network by opening the cascade between networks 1 and 2. Call this  $G_1$ . Now measure the available gain of network 2 by opening the cascade between 1 and 2, and between 2 and 3. Use a signal generator of internal impedance equal to the impedance seen looking into the output of network 1 with the original signal generator connected to it. Call this  $G_2$ . This is done for each network in turn, the measurement being made each time with a signal generator having an internal impedance equal to that seen looking back towards the beginning of the cascade, the cascade being broken at the point of connection of the element

to be measured. Consider the product

$$G_1 \cdot G_2 \cdot G_3 \cdots G_n = \left( \frac{S_1}{S_g} \right) \cdot \left( \frac{S_2}{S_1} \right) \cdot \left( \frac{S_3}{S_2} \right) \cdot \cdots \cdot \left( \frac{S_n}{S_{n-1}} \right)$$

where  $S_n$  is the available output power of the  $n$ th network when measured as above, and  $S_g$  is the available generator power. Rearranging,

$$G_1 \cdot G_2 \cdot G_3 \cdots G_n = \frac{S_1 \cdot S_2 \cdot S_3 \cdots S_n}{S_g \cdot S_1 \cdot S_2 \cdots S_{n-1}}$$

$$= \frac{S_n}{S_g}, \text{ the available gain of the cascade.}$$

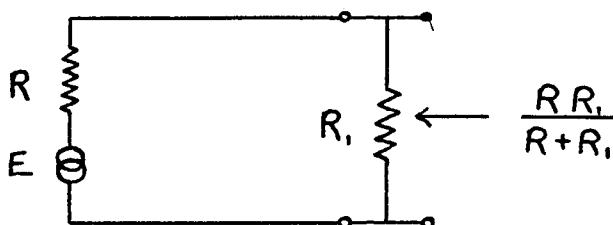
This result is valid only when the "available gain" of each element is measured with a signal generator whose internal impedance is equal to the impedance of the entire network preceding the element under measurement.

## 6. Nature of impedances considered

In all of the foregoing the impedances involved have been assumed real. For the remainder of this chapter it will be assumed that the reactances have been resonated at the frequency for which the analysis is made and that the impedances, therefore, will be real. The band of frequencies  $B$  is assumed to be centered at this frequency, and to extend only over a frequency band for which the impedances are substantially real and constant.

## 7. Available gain of a few typical networks

The first case is that of a resistor:





By Thévenin's theorem: Open circuit voltage =  $\frac{ER_1}{R+R_1}$

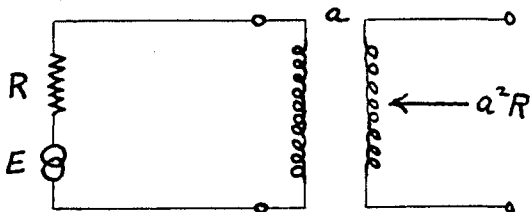
$$\text{Output impedance} = \frac{RR_1}{R+R_1}$$

$$\text{Available output power} = \frac{E^2 R_1^2}{(R+R_1)^2} \cdot \frac{4RR_1}{(R+R_1)}$$

$$\text{Available signal power} = \frac{E^2}{4R}$$

$$\text{Available gain} = G = \frac{\frac{E^2 R_1}{4R(R+R_1)}}{\frac{E^2}{4R}} = \frac{R_1}{R+R_1} = \begin{aligned} &= 1 \text{ for } R=0 \\ &= \frac{1}{2} \text{ for } R=R_1 \\ &= 0 \text{ for } R=\infty \end{aligned} \quad (1)$$

Ideal Transformer



We should obviously expect an available gain of unity

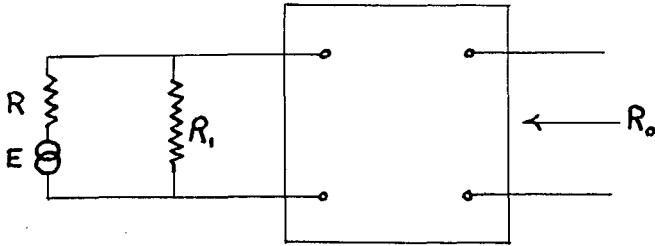
Output open circuit voltage =  $aE$

$$\text{Available output power} = \frac{a^2 E^2}{4a^2 R} = \frac{E^2}{4R}$$

$$\text{Available signal power} = \frac{E^2}{4R}$$

Therefore, available gain = 1 as expected

Shunted signal generator feeding an amplifier.



- Assumptions: (1) Infinite input impedance  
 (2) Open circuit voltage gain = A  
 (3) Output impedance =  $R_o$ , assumed to be independent of the impedances connected to the input.

$$\text{Available output power} = \frac{\left( \frac{A E R_i}{R + R_i} \right)^2}{4 R_o} \quad (2)$$

$$\text{Available generator power} = \frac{E^2}{4 R}$$

$$\text{Available gain} = G = \frac{\left( \frac{A E R_i}{R + R_i} \right)^2}{\frac{E^2}{4 R}} = \frac{R A^2}{R_o} \left( \frac{R_i}{R + R_i} \right)^2 \quad (3)$$

This result could be obtained by computing the separate "available gains" and taking their product as is shown below. From (1), the available gain for the resistor =  $\frac{R_i}{R + R_i}$

For the amplifier alone, supplied by a generator of arbitrary open circuit voltage E

$$\text{Available signal power} = \frac{\frac{E^2}{4 R R_i}}{R + R_i}$$

$$\text{Available output power} = \frac{(AE)^2}{4R_o}$$

$$\text{Available gain} = \frac{\frac{A^2 E^2}{4R_o}}{\frac{E^2 (R+R_i)}{4RR_i}} = \frac{A^2}{R_o} \left( \frac{RR_i}{R+R_i} \right)$$

$$\text{Product of two gains} = \frac{R_i}{R+R_i} \cdot \frac{A^2}{R_o} \cdot \frac{RR_i}{R+R_i} = \frac{A^2 R}{R_o} \left( \frac{R_i}{R+R_i} \right)^2$$

which checks.

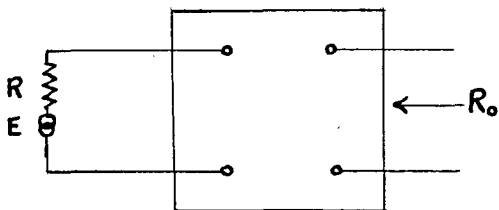
### 8. Noise figures of a few typical networks

In the first example we shall consider the circuit shown below in which an amplifier of open circuit voltage gain  $A$  is fed by a signal generator.

Assumptions: (1) Absolute temperature =  $T$  degrees

(2) Input impedance of amplifier =  $\infty$

(3) Amplifier is noise free



$$\text{Available signal power} = \frac{E^2}{4R}$$

$$\text{Available output power} = \frac{A^2 E^2}{4R_o}$$

$$\text{Available gain} = G = \frac{RA^2}{R_o}$$

Next compute "available output noise power"

$$\overline{E_n^2} = 4kTBR - \text{available from signal generator}$$

$$\overline{E_{no}^2} = 4kTBRA^2 - \text{open circuit mean-squared output voltage}$$

The "available output noise power" is obtained by dividing  $\overline{E_{no}^2}$  by  $4R_o$ .

$$N = \frac{4kTBRA^2}{4R_o}$$

but  $G = \text{available gain} = \frac{RA^2}{R_o}$

therefor  $N = GkTB$  (5)

The "available output signal power" however, is  $S = GS_g$  where  $S_g$  is the "available signal power". The suggestion is strong, therefore, that  $kTB$  be considered the "available noise power" from the generator which it may be if the meaning assigned to it in Section 3 is used.

Now noise figure is defined as

$$F = \frac{\text{input available signal to available noise power ratio}}{\text{output available signal to available noise power ratio}}$$

Symbolically,

$$F = \frac{\frac{S_g}{kTB}}{\frac{S}{N}} \quad (6)$$

The above definition shows clearly that the noise figure is not a measure of the excellence of the output signal-to-noise ratio, but merely a measure of the degradation suffered by the signal-to-noise ratio as the signal and noise pass through the network in question. A noise free amplifier would, of course, have a noise figure of 1 since the signal-to-noise power ratio would be unaltered in passing through it.

For the above example:

$$F = \frac{\frac{S_g}{kTB}}{\frac{GS_g}{GkTB}} = \frac{S_g}{S_g} = 1 \quad \text{which is the expected}$$

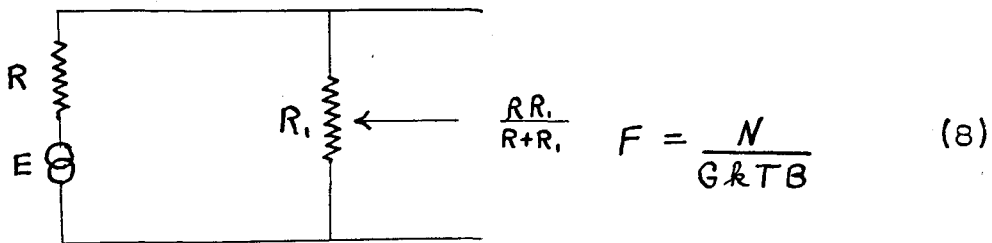
result since the amplifier was assumed to be noise free.

(6) may be rearranged to give

$$N = \frac{S}{S_g} FkTB = FGkTB \quad (7)$$

In other words the "available output noise power"  $N$  is the product of  $GkTB$  and the noise figure.

Having already computed the "available gain" of a resistor, it is interesting to compute the noise figure of a resistor



$N$  = available output noise power

= open circuit mean-squared output voltage of circuit  
4 . output impedance

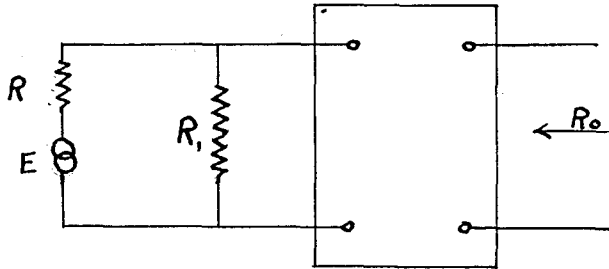
$$= \frac{\frac{4kTBRR_1}{R+R_1}}{\frac{4RR_1}{R+R_1}} = kTB \quad (\text{a result known by definition})$$

Since  $G$  for a resistor =  $\frac{R_1}{R+R_1}$ ,

$$F = \frac{\frac{kTB}{\frac{R_1}{R+R_1}}}{kTB} = \frac{R+R_1}{R_1} \quad (9)$$

where  $R$  is the generator impedance and  $R_1$  the value of the resistor.

Now compute the noise figure of a generator, a resistor, or, and a noise free amplifier.



$$N = \frac{4kTBRR_1A^2}{(R+R_1)4R_o} = \frac{RA^2R_1kTB}{R_o(R+R_1)}$$

$$G = \frac{RA^2}{R_o} \left( \frac{R_1}{R+R_1} \right)^2$$

$$F = \frac{\frac{RA^2R_1kTB}{R_o(R+R_1)}}{\frac{RA^2}{R_o} \left( \frac{R_1}{R+R_1} \right)^2 kTB} = \frac{R+R_1}{R_1} \quad (10)$$

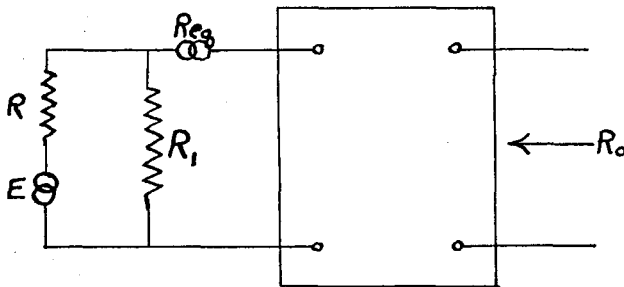
This is the same as for a resistor above, which is what we expected since we assumed a noise-free amplifier.

#### 9. Consideration of "equivalent noise resistance" $R_{eq}$ .

The next computation of noise figure involves a generator, a resistor, and a noisy amplifier. It is now common practice to use the concept of the "equivalent-resistance" method for characterizing noise in an amplifier and it will be used here. In cases where a complex noise source can be represented by one equivalent noise source, it is

convenient to represent the noise by a fictitious generator which, when inserted in the circuit will produce the same noise output from a noise-free network as that produced by the noisy network. Such a fictitious generator has its voltage specified in terms of a resistor, generally at room temperature, which produces the required noise voltage and which is termed the "equivalent noise resistance",  $R_{eq}$ . This concept is most used with networks involving tubes, crystal rectifiers, and other devices which have noise in excess of that which can be directly attributed to the Johnson effect alone. It is necessary to exercise care in the use of this concept, since a complex noise source may be replaced by a single noise source only under carefully restricted conditions. It is a convenient concept for use with vacuum tubes since North (19) and his co-workers have done extensive work on the problem and have derived formulas for the calculation of the "equivalent noise resistance" for many tube types. Tables of values for commonly used tube types are included in Valley (20). In the case of triodes, the concept is applicable only in the absence of feedback and transit-time effects. If either or both of the above are present, additional noise sources are necessary to represent the noise behavior. In the case of tetrodes or pentodes, the use of a single equivalent noise source additionally requires that the screen and suppressor be returned directly to the cathode. It must, moreover, be realized that

the use of a single noise source to represent a complex noise source implies some rather drastic assumption concerning the frequency behavior of the impedances associated with the actual noise sources. Despite all of these restrictions, however, the concept leads to many useful results.



- Assumptions (1) Open circuit voltage gain = A  
 (2) Noise bandwidth = B  
 (3) Infinite input impedance  
 (4) Output impedance =  $R_o$

Mean-square noise voltage of  $R_{eq} = 4kTB R_{eq}$

$$\text{Available gain} = G = \frac{RA^2}{R_o} \left( \frac{R_1}{R+R_1} \right)^2, \text{ from (3)} \quad (11)$$

Available output noise power = N

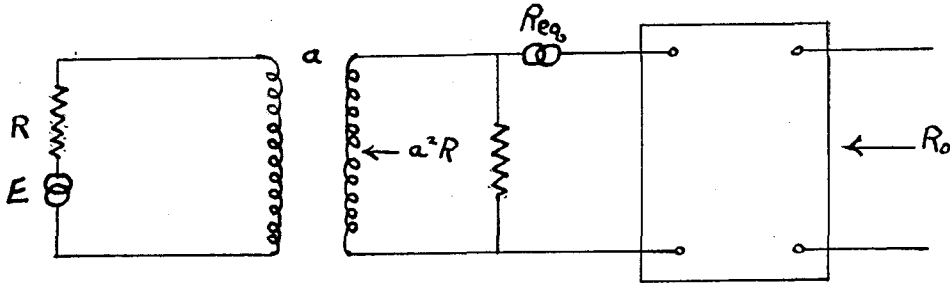
$$N = \frac{4kTB A^2}{4R_o} \left( R_{eq} + \frac{RR_1}{R+R_1} \right) \quad (12)$$

$$\begin{aligned} F &= \frac{N}{GkTB} = \frac{4kTB A^2}{4R_o} \left( R_{eq} + \frac{RR_1}{R+R_1} \right) \\ &\quad \frac{kTB R A^2}{R_o} \left( \frac{R_1}{R+R_1} \right)^2 \\ &= \frac{R_{eq}}{R} \left( \frac{R+R_1}{R_1} \right)^2 + \frac{R+R_1}{R_1} \end{aligned} \quad (13)$$



It is well to make a few observations in connection with (10) and (13), viz, (1) If  $R_{eq} = 0$ ; (13) reduces to (10) as it should; (2) If  $R_1$  may be assigned arbitrarily, the noise figure is best if  $R_1$  is made large without limit and, (3) If  $R_1$  is sufficiently large, the noise figure is improved by making  $R$  larger.

In the usual case we are forced to seek the optimum noise figure with fixed values of  $R$  and  $R_1$ . Hence we shall consider the use of an ideal transformer between generator and  $R_1$  to improve the noise figure. In practice this may take the form of an ordinary transformer, an autotransformer or the  $\pi$  and T equivalents.



$F$  may be written directly from (13) by realizing that the generator and transformer are equivalent to a new generator of internal impedance  $a^2 R$  and open-circuit voltage  $aE$ . Substituting  $a^2 R$  for  $R$  in (13)

$$F = \frac{R_1 + a^2 R}{R_1} + \frac{R_{eq}}{a^2 R} \left( \frac{R_1 + a^2 R}{R_1} \right)^2 \quad (14)$$

To find the value of  $a$  for minimum  $F$ , we take the derivative of  $F$  with respect to  $a^2$  and equate to 0. The resultant value of  $a$  for minimum  $F$  is then

$$a^2 = \frac{R_1}{R\sqrt{1 + \frac{R_1}{R_{eq}}}} \quad (15)$$

It should be noted that the condition for optimum noise figure is not a match between generator and  $R_1$ . Such a condition would make  $a^2 = R_1/R$ . The condition for optimum noise figure is a mismatch in which the optimum transformation ratio transforms the generator impedance to a value somewhat less than the resistance of  $R_1$ . The degree of mismatch involved is a function of the noisiness of the amplifier and the condition approaches that of match only when the amplifier is extremely noisy or when  $R_1$  is very small. Such might be the case for a multigrid mixer used at broadcast frequencies. For well designed input circuits in receivers,  $R_1/R_{eq}$  is not negligible and the mismatch is important if optimum noise figure is to be obtained.

#### 10. Consideration of the partition of the available output noise power.

In an examination of the "available output noise power"  $N$ , equal to  $FGkTB$ , the question is raised as to the relative contribution to  $N$  of noise from the signal generator and noise from the network. Since the "available noise power" from the generator is  $kTB$  and the "available output noise power" due to the generator is  $GkTB$ , it follows that the contribution from the network alone is

$(F - 1)GkTB$ . It should be realized that  $F$  is a function of  $T$ , and is completely specified only when  $T$  is given. It is, moreover, implicit in the definition of noise figure, that all noise sources be referred to the same temperature. A standard temperature for noise figures has been suggested and most suggestions approximate room temperature. Friis (4) has suggested 290°K, and 288°K has also been suggested. The latter figure leads to a much simplified result in the measurement of noise figures by means of "noise diodes", as will be shown in Chapter V. In any case it should be remembered that all noise source must be referred to the same temperature. The importance of this is shown in the following section.

11. Consideration of the effect on noise figure of a temperature difference between the antenna and the other networks of the receiver.

From Section 10 we know that all noise sources must be referred to the same temperature and in all of the present chapter we have considered this temperature to be room temperature. A radar receiver so measured, however, is ultimately used with a directive antenna which, when pointed at space for instance, may have an effective temperature well below room temperature. The signal-to-noise degradation due to the receiver in this case will be greater than indicated by the conventional noise figure. It is important, therefore, to consider the derivation of an effective noise figure for such a case. At the outset the noise figure of any network

measured and referred to a temperature  $T$  will be written

$$F_T = \frac{N}{GkTB} \quad (16)$$

where the subscript  $T$  denotes the fact that the generator and network are at the temperature  $T$ . The "available output noise power" due to the network alone, at the temperature  $T$ , is  $(F_T - 1) GkTB$ . If a generator at temperature  $T_g$  is connected to a network at temperature  $T_n$ , the "available output noise power" is

$$N = GkT_g B + (F_n - 1) GkT_n B \quad (17)$$

Defining the effective noise figure,

$$F_{eff} = \frac{N}{GkT_g B} \quad (18)$$

we obtain

$$\begin{aligned} F_{eff} &= \frac{GkT_g B + (F_n - 1) GkT_n B}{GkT_g B} \\ &= 1 + \frac{T_n}{T_g} (F_n - 1) \end{aligned} \quad (19)$$

## 12. Consideration of noise figure of various amplifier configurations.

In his article on noise figure, Goldberg (5) uses the foregoing procedures to obtain the noise figures of amplifiers of the three basic configurations namely; grounded cathode, grounded grid, and grounded plate amplifiers. Suprisingly enough the noise figures of the three configurations are identical which leads the author to the conclusion that;

The noise figure of an effective three-element amplifier tube is essentially independent of the manner of its connection into the circuit, i.e., whether it be connected in conventional fashion, as a grounded grid stage, or as a cathode follower.

The fact that the noise-figure formulas are identical does not, however, mean that the circuits can be considered as interchangeable from a noise standpoint. The reasons for this are associated with the circuits to be used with the amplifier and will be considered in Section IV in the design of a low noise amplifier.

## CHAPTER III

### CONTRIBUTIONS TO NOISE IN MICROWAVE RECEIVERS

#### 1. General

It is well known that despite our ability to amplify a feeble electrical signal by practically any desired factor, it is still not possible to discern an arbitrarily weak signal because of the presence of random electrical fluctuations or "noise". If the true signal entering any receiver is made weaker and weaker, it must eventually subside into the fluctuating background noise and be lost.

A consideration of the origin of these fluctuations seems to be in order as do the factors which determine precisely the level at which the signal is obscured by them.

As a preliminary to the answers to these decisive questions, it is worth while to consider briefly the limit of useful sensitivity of an ordinary low frequency radio receiver. This limit is also set by the level of random disturbances, but in this case the random disturbances with which the signal must compete originate generally not in the receiver itself but elsewhere in space. The source of such noise may range from man made noise from a passing trolley to the mysterious atmospheric noises of interstellar space, but in any case they enter the receiver by way of the antenna. The crucial quantity, therefore, is the ratio of the field strength of the signal in the neighborhood of the antenna to that of noise or interference.

Hence we see that the absolute magnitudes of signal and interference power available at the antenna terminals are of little importance, the ratio determining the ultimate performance.

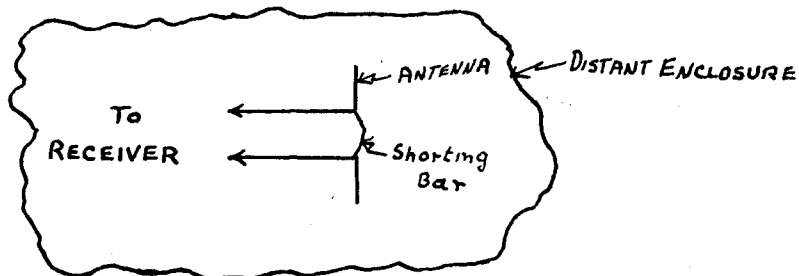
The situation is different in the microwave region. Here, substantially all the noise originates in the receiver itself; not because microwave receivers are noisier or less perfect receivers than low frequency receivers, but because noise and interference originating outside the receiver are enormously greater at the lower frequencies. It can be said, in fact, that such noise in the microwave region is almost entirely negligible in existing radar receivers. The noise against which the signal must compete for recognition is, therefore, that noise which originates in the receiver itself. It is this noise which will be treated in this paper, with particular emphasis on the noise in the intermediate frequency (pre) amplifier.

## 2. Antenna noise

There has always been considerable speculation as to whether the radiation resistance of an antenna should be regarded as a source of thermal noise, and if so what temperature should be attributed to it. In terms of the mechanism of thermal noise in a metallic resistor, there was no reason to expect an additional noise contribution due to the radiation resistance; but it has since been proved that the radiation resistance of an antenna is a source of thermal noise, of magnitude indicated by Nyquist's formula, and at

some temperature  $T_r$ . The value of  $T_r$  varies from  $0^\circ$  Kelvin in free space to the temperature of the space surrounding the antenna if the antenna is in an enclosure at a uniform temperature.

In a practical case, the difficulty in determining this effective temperature of the radiation resistance is the sole obstacle in the way of calculating the thermal noise developed. To get at the heart of the problem, we shall first show that the noise power of the radiation resistance originates not in the antenna but in its surroundings, whether near or distant, which are capable of radiating power to it. To demonstrate this, consider the idealized antenna shown below, which has radiation resistance but no ohmic resistance. Consider the case where the antenna is not connected to any circuits



(shorting bar in place). In this case, if  $i_r$  is the antenna current (at its mid-terminal), the antenna will receive power of amount  $i_r^2 R_r$ , where  $R_r$  is the radiation resistance, and radiate power of the same amount. The antenna thus is not the source of any power but merely acts to reflect or scatter the power that comes to it from the outside. If the antenna has ohmic resistance



$R_0$ , then it will generate a thermal-noise voltage  $4kTBR_0$  of its own; but in the absence of such ohmic resistance, the antenna will not be the original source of any thermal-noise power.

If now the antenna is connected to a receiver, it will deliver some of the thermal-noise power that it receives from the outside to the receiver. The amount of noise power that it delivers can be determined by assuming that it is a source of voltage whose mean-squared value is

$$\overline{e^2} = 4kR_pT_sB$$

where  $T_s$ , the mean thermal temperature of the radiation resistance, is an average temperature of the antenna's surroundings which are capable of radiating power to it. In estimating the average, the directions of these surroundings must be considered with respect to the directivity of the antenna. Hence  $T_s$  is a kind of weighted average of the earth's surface temperature and the effective temperature of the radiating surroundings. At lower frequencies,  $T_s$  is much greater than room temperature, reaching values of 1,000 times as great under unfavorable conditions. At the higher frequencies, particularly above 50 Mc., it declines, but it continues to be somewhat greater than room temperature. From this we can see that the thermal noise generated in the radiation resistance of the antenna is in any case of considerable magnitude.

### 3. Crystal converter and local-oscillator noise

The noise temperature of any device is defined as the

ratio of the noise power available from the device to that available from a resistor at room temperature. The noise temperature of a crystal converter is never less than unity. By definition, it would be unity if no excess noise were developed in the crystal itself and the noise power available from the converter were only the Johnson noise associated with the output admittance of the crystal converter at the intermediate frequency. If the conversion loss of the unit were very small, the i-f admittance would have a temperature determined by the objects and absorbing media in the field of view of the antenna. When the noise temperature of a converter is measured, however, the antenna is replaced by an r-f resistance at room temperature and, if no excess noise were developed in the converter, the noise power available from the converter would be  $kTB$  where  $T$  is room temperature.

As a result of the research on semiconductor crystals and on the techniques of preparation and manufacture of rectifier units, the noise temperature of crystals now available has become much smaller than that of early units. The excess noise developed by a crystal unit is associated with the flow of current through the barrier; the current flow consists of a flow of discrete charges and, consequently, has a nonuniform character. The approximately linear relationship between the noise temperature of the converter and the crystal current, which is roughly proportional to the incident-local-oscillator power, bears out the theory that

the noise is similar to the shot effect noise in a diode.

In order to specify the quality of a crystal as a converter, it is necessary that the conversion loss and the noise temperature correspond to the same local oscillator power. The magnitude of local oscillator drive should be chosen to be that magnitude which produces the best over-all noise figure for the receiver in which the crystal is used as a converter. The optimum local oscillator power depends on the noise figure of the i-f amplifier which follows the converter. The local-oscillator drive chosen for the specification of the loss and noise temperature is that which results in the minimum over-all noise figure in a receiver using an i-f amplifier with a noise figure typical of present production. If the i-f amplifier has a smaller noise figure, the optimum value of local-oscillator drive for best noise figure is less. For best results in any case, the optimum local-oscillator drive should be determined experimentally.

It has been found that the noise temperature of a crystal converter is not independent of the intermediate frequency at which it is measured. In general, it is found to be lower at high intermediate frequencies than at low ones, although this effect is not very pronounced at frequencies above a few megacycles per second. The maximum acceptable noise temperatures for various crystals for an intermediate frequency of 30Mc/sec are given in Pound (16) and vary from 1.5 in some of the later

crystals to 4 in the 1N21. If one considers that with an i-f amplifier having a noise figure of unity, a change in the noise temperature, ideally equal to 1, by a given factor produces a change in the over-all noise figure by the same factor, it is easy to see the importance of keeping the noise temperature small. This becomes particularly important in amplifiers with noise figures of the order of 1.3 - 1.4 of the type to be discussed in Chapter IV.

The subject of local-oscillator noise is closely connected with crystal converter noise and hence is considered at this time. Spurious signals accompanying the local-oscillator signal are called "local-oscillator noise". The effect of these spurious signals has been found to be negligible below 3000 Mc. but of considerable importance at higher frequencies, particularly when low intermediate frequencies are used.

The electron beam passing through the oscillator cavity contains noise-current components of all frequencies, because it is made up of discrete electronic charges. In fact, if a klystron oscillator tube is operated at a reflector voltage that does not cause it to oscillate, a noise spectrum can be detected in its output circuit. The noise voltage in the output circuit is, of course, largest at the resonant frequency of the cavity, because the coupling to the electron beam is most efficient at this frequency. Such oscillators, operated in this way, have been used

as noise generators in the measurement of over-all noise figures of microwave receivers.

If, on the other hand, the klystron is oscillating, it is reasonable to expect that the noise voltages in the output circuit as a result of the spurious frequencies will be the same at frequencies on either side of the oscillation frequency.

In addition, low-frequency noise components in the electron beam may, through amplitude or frequency modulation of the oscillator signal, produce noise sidebands above and below that of the oscillator signal. These sidebands will be coupled to the output circuit with decreasing efficiency at frequencies removed increasingly far from the resonant frequency of the oscillator cavity. In view of the above, the oscillator may be expected to have a noise spectrum in its output circuit similar to that shown below.

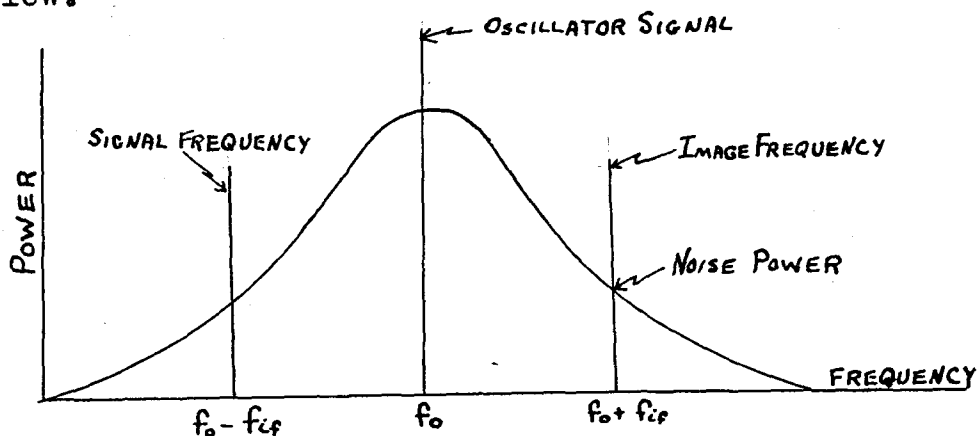


Fig. 1 - Local-oscillator noise as a function of frequency.

The question of how much deterioration the local-oscillator noise causes in the receiver noise figure depends upon the local-oscillator noise power at the signal and image

Frequencies. For a low frequency receiver and, for example, a 30Mc./sec intermediate frequency, the loaded  $Q$  of the oscillator cavity is usually sufficiently high to reduce the signal-and image-frequency noise components from the local oscillator to a negligible level. It is obvious from the preceding curve that an increase of receiver frequency, hence local oscillator frequency, with no change in the intermediate frequency will result in a reduction of the filtering action of the local-oscillator cavity. To maintain the same filtering effect with a constant oscillator cavity  $Q$ , it is necessary to match the increase in local-oscillator frequency by a proportionate increase in the intermediate frequency.

It follows from the above that the presence of a significant amount of local-oscillator noise may influence the choice of an intermediate frequency. Especially for receivers at 9000Mc/sec and above, the selection of an intermediate frequency has involved a choice between the reduced local-oscillator noise at high intermediate frequencies, on the one hand, and the lower amplifier noise at low intermediate frequencies on the other hand. The application of such considerations in the actual design of a receiver will be treated in the section on reduction of noise external to the amplifier.

#### 4. Thermal agitation noise of input resistance.

The free charge of any conductor is in random motion in equilibrium with the thermal motion of the molecules of

the conductor and this flow of charge creates a random voltage across the terminals of the conductor. The relation among the mean-square fluctuation voltage  $\overline{V}^2$  between the terminals of a material conductor (i.e. not thermionic, but metallic, electrolytic etc.), the resistance  $R$ , and absolute temperature  $T$  of the conductor is

$$\overline{V}^2 = 4RkTB \quad (29)$$

Formula (29) has been verified by Johnson (9), Sandeman (17) and Moullin (12) and has been theoretically interpreted both in terms of thermodynamics and of the mechanism of metallic conduction.

Since  $\overline{V}^2 = R^2 \overline{I}^2$ , it is legitimate to replace formula (29) by

$$\overline{I}^2 = \frac{4kTB}{R} \quad (30)$$

where  $\overline{I}^2$  is the mean-square fluctuation current flowing through the resistor  $R$ . Since Nyquist's paper was published it has been found possible to deduce (30) from the mechanism of electronic conduction in a metal, Bell (1). It is well known that a flow of current through a metallic conductor represents a small uniform drift velocity superimposed on the large thermal-agitation velocity of the conduction electrons; but each of the individual electron movements due to thermal agitation forms a component of the fluctuation current, the observed fluctuations being in fact the resultant of all the thermal-agitation movements of the electrons

within the conductor. The number of electrons and their mean free path can be eliminated in terms of the resistance of the conductor, so that the fluctuation current comes out as a function of the resistance and of the thermal energy  $1/2kT$  of each electron, giving in fact equation (30).

Having once been established for a particular mechanism of conduction, this equation can be extended to any other type of conductor having a known temperature and resistance by the thermodynamic argument of the necessity of energy equilibrium between two bodies at the same temperature, one being a metallic resistor and the other a resistor in which the mechanism of conduction is not amenable to detailed calculation.

## 5. Shot effect and flicker effect

Early in the study of noise in vacuum tube amplifiers Schottky (18) showed that under certain conditions a noise is produced which depends on the fact the electric current is a flow of discrete particles, the electrons, which are emitted from the cathode in a random manner. This random electron emission produces a statistical current fluctuation in the tube and coupling impedance. This fluctuation, called the "shot effect", appears as noise in the output of the amplifier. In a temperature-limited diode the current consists of a large number of current impulses of equal magnitude but occurring at random intervals of time; each current impulse, representing the transit of one electron, commences abruptly



as the electron leaves the cathode and terminates equally abruptly as it arrives at the anode, the duration of the whole pulse being small compared with the period of the highest frequency used for observation. By taking a Fourier series over a period long compared with the time of observation, the resultant of all the electron transits can be analyzed into a mean current  $i$  and a fluctuating component of which the mean-square value is given by

$$\overline{I^2} = 2ieB$$

Because this formula is so well established, the temperature-limited diode is a convenient source of truly random fluctuation current of known magnitude, covering a very wide region of the radio-frequency spectrum. This characteristic of temperature-limited diodes is very useful in the design of a noise generator as will be shown in a later section. The above expression holds quite accurately for tubes in which the cathode is either clean or thoriated tungsten. When an oxide-coated cathode is used, fluctuations of a larger magnitude are superimposed on the true shot effect. This disturbance has been attributed to a state of flux and change in the activating material on the surface of the cathode and is called "flicker effect". It is not, however, of concern above about 10 Kc. and will not be considered further.

The treatment of shot effect in space-charge-limited diodes or equivalent negative grid triodes is subject in general to two separate and distinct schools of thought.

On the one hand, Bell (1) holds to the conviction that thermal noise and space-charge-limited shot noise are two limiting cases of the same general phenomenon associated with electrical conductors while others such as Llewellyn (11) Moullin (12), and Williams (22) worked on the hypothesis that the effect of space charge was to reduce the current fluctuations of shot effect by variable factor A, for which there was as yet no theoretical explanation, and that Nyquist's theorem did not apply to a vacuum tube.

There have been over a hundred articles written in the past thirty years in an attempt to establish the final nature of space-charge limited shot effect and the search is still underway. Good bibliographies are contained in Johnson (10) and Bell (1). For the purpose of this paper, it is sufficient to recognize (1) that it does exist, (2) that its effect varies for varying degrees of space charge, and (3) that it varies for various tube configurations. In connection with (3) it is important to consider the additional complications introduced by the tetrode and pentode which contain two or more current collecting electrodes. Usually one of these is the anode proper while the other is a screen of more or less open mesh through which the electron stream must pass before reaching the anode. The question whether a particular electron will pass through a close-mesh positively-charged screen or be collected

by it depends partly upon the transverse component of its velocity, which is of thermal origin and therefore random. Ziegler (23) assumed that although the ratio of mean anode current to mean screen current was fixed, the probability of any particular electron going to one or the other was a purely random function, and that this random partition of current introduced a fluctuation current which gave rise to an additional noise known as partition noise. This explains why a tetrode or pentode gives higher values of shot effect noise than does a triode.

There are, of course, other sources of noise such as vibration, poor contacts, poor insulation, faulty resistances and gassy tubes. It is possible, however, by quality control to either eliminate these entirely or to so reduce them as to make their contribution negligible.

## CHAPTER IV

### REDUCTION OF NOISE IN RECEIVERS

#### 1. Noise external to the i-f amplifier.

The last chapter was devoted to a treatment of the sources of noise power in receivers generally, both internal and external. The present section is a discussion of the methods used to reduce the noise power to the least possible value.

It has been pointed out that atmospheric and man made noises can be greatly reduced by the use of highly directive antennas and experience has shown that the effect of such noise sources is negligible in microwave receivers. Since it is such receivers with which we are concerned, it is unnecessary to consider this source further. The noise power developed in the radiation resistance of the antenna is a source which cannot be eliminated. Since, however, the noise figures of receivers are considerably greater than unity, the output noise power of the receiver which arises from the antenna resistance is small for an apparent antenna temperature near room temperature.

The reduction of crystal noise (effective temperature) is a function of crystal design. For a particular application the selection of the best crystal to use is based on several parameters, the most important of which are conversion loss and noise temperature. It is, of course, desirable that both these parameters be as small

as possible and the two considered together determine the quality of the crystal. In the 10 centimeter band we find the 1N21 series of crystals with maximum conversion losses ranging from 8.5 db in the 1N21 down to 5.5 db in the 1N21C and with maximum noise temperatures ranging from 4 times in the 1N21 down to 1.5 times in the 1N21C. The same general trend is true in the 3 centimeter and 1 centimeter bands and the design of a receiver should be such as to utilize the properties of the best crystal available at the time.

The most effective and widely used method of reducing local-oscillator noise is the use of a microwave balanced mixer. Such a mixer utilizes two separate mixer units driven in shunt by the local-oscillator signal and in push-pull by the received signal, or vice versa. This results in a balanced push-pull output signal at the intermediate frequency, and the i-f amplifier input circuit is designed to give response only to such a balanced signal. Any i-f output signals derived from noise accompanying the local-oscillator power appear in the same phase at the output terminals of each mixer unit and are therefore discriminated against by the input circuits of the push-pull i-f amplifier.

The figure below is a schematic drawing of a microwave balanced mixer. If it is assumed that

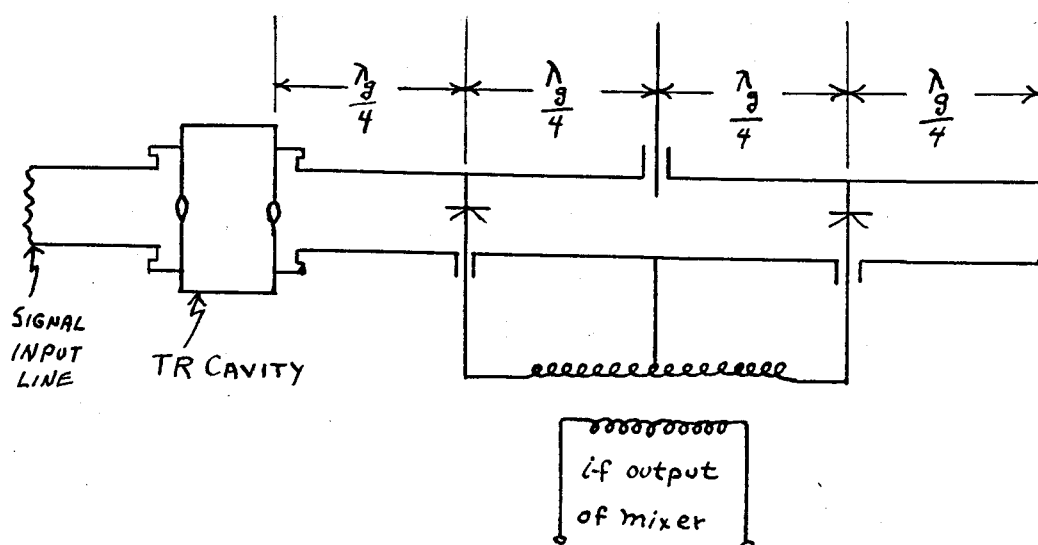


Figure 2  
Simple balanced mixer with push-pull i-f transformer  
to unbalanced line

the crystals may be treated as resistors across the microwave line and that the local-oscillator power can be introduced into the microwave line by a simple, very loosely coupled probe, it can be seen that the circuit behaves as a balanced mixer. The TR cavity is assumed to present a short circuit to power at the local oscillator frequency. Each crystal is, therefore, coupled to the local oscillator in the same way and, since the probe excites travelling waves in both directions and having the same phase at planes equi-distant from the probe, the local-oscillator signals at the two crystals are in phase. The received signal, on the other hand, having passed through the TR cavity, arrives at the two crystals in the opposite phase since the crystals are spaced one-half wavelength apart. A consideration of the addition of a small signal wave and a large local-oscillator wave will show that the amplitude-modulation component at the beat frequency,

in the envelope of the sum of these two waves, reverses in phase if the relative phases between the local oscillator wave and the signal wave are reversed. Thus the i-f voltages at the output terminal of the two crystals are opposite in phase. By means of the transformer, the push-pull i-f signal is changed into a signal that can be used to excite a conventional unbalanced line or an i-f amplifier.

Local oscillator noise reaches the two crystals through the same circuit as does the local-oscillator signal. The relative phases between the noise components and the local-oscillator wave are the same at the two crystals, and therefore the noise converted to the intermediate frequency has the same phase at the output terminals of the two crystals. The balanced transformer does not produce an output voltage from equal voltages in the same phase in the two legs of its input circuit, and thus the converted noise is not coupled into the i-f amplifiers. Balanced mixers in use vary considerably from the schematic shown but in all of them the local-oscillator noise power is eliminated by some such cancellation.

## 2. Internal intermediate frequency amplifier noise

In the final analysis, it is the noise power output of the i-f amplifier which sets the lower limit to the overall noise figure of the receiver. All efforts to reduce the noise power originating in the antenna, crystal converter, and local-oscillator are futile if

the noise figure of the i-f amplifier is not kept at a low value.

It has been pointed out in Chapter III that the random division of cathode current between plate and screen in a pentode makes the shot-noise current of a given pentode much greater than that of the same tube connected as a triode with screen strapped to plate. According to Thompson (19) the ratio of shot noise currents in the two cases is of the order of 3 to 5 times. This effect is called "partition noise"; because of it many suggested arrangements for obtaining good amplifier noise figure have revolved around the use of a triode as a first stage.

In Chapter II, it was pointed out that the noise figure of an effective three element amplifier tube is essentially independent of the manner of its connection into the circuit, i.e., whether it be connected as a grounded cathode, a grounded grid, or as a cathode follower. This noise figure is

$$F = \left( \frac{R_s + R_g}{R_g} \right) + \frac{R_{eq}}{R_s} \left( \frac{R_s + R_g}{R_g} \right)^2 \quad (32)$$

A statement was also made, without explanation, that the equality of noise figure formulas did not mean that these circuits were interchangeable from a noise standpoint for reasons associated with the circuits to be used with the amplifier. Some of these reasons are treated in the following two paragraphs.



Consider the problem of stability. It is well known that the grounded-cathode triode amplifier is prone to oscillation unless neutralized. For this reason, a pentode would normally be preferred except that pentodes are generally noisier than triodes. To obtain stability, the grounded-grid amplifier has become popular in recent years. The cathode-follower may be used but generally is not.

The remaining considerations can best be separated on the basis of whether or not the input source must be matched, and upon a consideration of the noise figure of the second stage. If a match to the source is desired, the noise figures for the grounded-cathode amplifier and the cathode follower are identical.  $R$  must be used to terminate the line and the noise figure becomes

$$F = 2 + 4 \frac{R_{eq}}{R_s} \quad (33)$$

By the use of a transformer between generator and termination,  $R$  may be made large, the limit being set by the type of transforming network used and the bandwidth required. In the case of the grounded-grid amplifier, however, the dynamic impedance may be arranged to terminate the line by choosing a tube with proper  $g_m$  and plate load. Thus, in the grounded-grid amplifier, the line or source may be matched even though  $R$  is infinite. The noise figure for this condition is

$$F = 1 + \frac{R_{eq}}{R_s} \quad (34)$$

The problem is not completely definitive, however, since the noise figure of the following stage must be considered. Moreover,  $R$  may generally be made high in the conventional amplifier by means of a transformer, but not in the grounded grid case because of voltage-gain reasons. Nevertheless the grounded-grid amplifier may be a good choice where low noise figure and line termination must be achieved simultaneously. The cathode follower is not generally used because of the lack of voltage gain from grid to cathode.

### 3. Consideration of a low-noise amplifier

In any study of low-noise amplifier design, the student is sooner or later referred to the Wallman amplifier. It is with this amplifier, and with slight variations of it, that the writer has worked, and it is the circuit discussed in this section.

The arrangement in question was devised by Wallman, Macnee, and Gadsden in 1944 at the M.I.T. Radiation Laboratory. It consists of a grounded-cathode triode first stage, followed by a grounded-grid triode second stage. An a.c. diagram is shown in Fig. 3. The various coils are midband resonant with their associated capacitances.

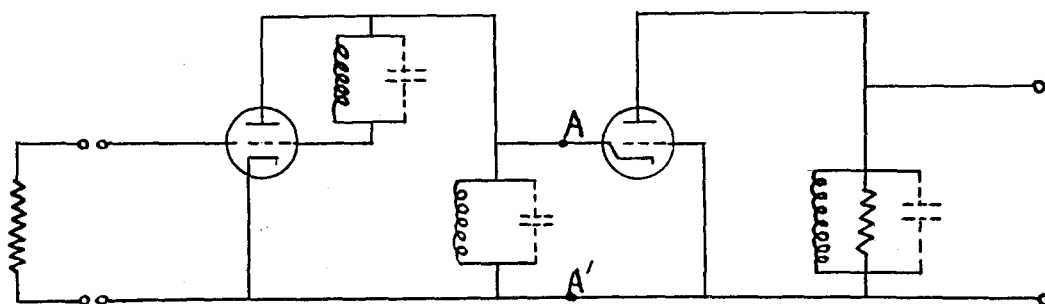


Figure 3  
A.c. diagram of cascode low-noise amplifier.

The coil  $L_n$  in parallel with the grid-plate capacitance  $C_{gp}$  is a neutralizing coil whose main purpose is, however, not to obtain stability but to achieve low noise figure. It is not critical, as shown by the fact that stability is preserved if it is omitted entirely, and the noise figure is degraded only 0.2 db at 30 Mc.

The grounded-cathode, grounded grid combination is designated "cascode" by its originators. It provides (a) the stability and noncriticalness of a pentode, (b) the amplification and gain of a pentode, and (c) the low noise figure of the first triode. It is the two triodes together that have the amplification of a single pentode and the cost of the improvement in noise figure is one additional tube. Conventional pentode amplifier stages follow the cascode to provide the bulk of the gain. A typical i-f pre-amplifier employing the Wallman circuit is shown in Fig. 6.

For use in the subsequent discussion, we now consider the noise figure analysis of a grounded-cathode amplifier stage. The analysis is made at midband frequency, at which the various tube and circuit capacitances are assumed to be resonated out. The amplifier can then be analyzed in terms of the equivalent circuit of Fig. 4.

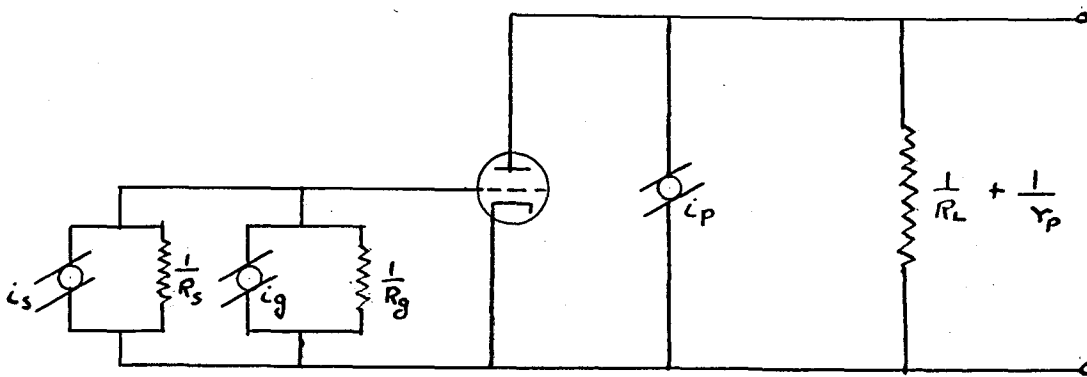


Figure 4  
Constant current equivalent circuit for noise figure analysis

Following the lines of the development of noise figure in Chapter II, we consider the noise figure of the above circuit. From equation (3) we find

$$\text{Available gain} = \frac{R_s \mu^2}{r_p} \left( \frac{R_g}{R_s + R_g} \right)^2 \quad (35)$$

From equation (13) we find

$$\text{Noise figure} = F = \frac{R_s + R_g}{R_g} + \frac{R_{eq}}{R_s} \left( \frac{R_s + R_g}{R_g} \right)^2 \quad (36)$$

It will be recalled from Chapter II that it is common practice in noise-figure analysis to replace an actual tube with plate circuit noise current  $i_p$  by a fictitious noiseless tube having in series with its signal grid a noise voltage  $e_{eq} = i_p / g_m$ . It is then possible to define  $R_{eq}$  according to the relation

$$R_{eq} = \frac{\overline{e_{eq}^2}}{4kTB} \quad (37)$$

Equation (36) for noise figure neglects the effect of transit-time loading and must be corrected for the

operating frequency. For transit angles less than one radian, corresponding to frequencies less than 200 Mc. for 6AK5, it has been determined by North (13) that the effects of electron-transit-time can be represented by a shunt resistance  $R_t$  from grid to cathode in parallel with a noise current  $i_t$  such that

(a) the ratio  $T_t$  of  $\overline{i_t^2}$  to  $4kB/R_t$  is constant, that is independent of frequency, and

$$(b) \quad T_t \doteq 5T \quad (38)$$

This representation assumes that transit-time grid noise is statistically independent of plate noise, or, in any case, that the effects add in the mean square. This is not correct for large transit angles but for the present 30 Mc. case involving a 6AK5, it is very good.

In any carefully designed 30 Mc. amplifier, input loading due to circuit losses can be kept so low as to have negligible effect on amplifier noise as compared with transit-time loading. Moreover, because of its high effective temperature, the effect on noise figure of transit-time loading completely dominates that of circuit losses. For this reason, in the following discussion of noise performance, the grid loading can be assumed to consist of transit-time loading only, and  $i_g$  to be equal to  $i_t$ . The noise figure of the circuit of Fig. 4 is

$$F = 1 + \frac{\overline{i_g^2}}{\overline{i_s^2}} + \frac{\overline{i_p^2}}{\overline{i_s^2}} \left( \frac{R_s + R_g}{R_s R_g} \right) \frac{1}{g_m^2}$$

or substituting

$$F = 1 + \frac{4kBT_g}{\frac{R_g}{\frac{4kTB}{R_s}}} + \frac{g_m^2 R_{eq} 4kTB}{\frac{4kTB}{R_s}} \left( \frac{R_s + R_g}{R_s R_g} \right)^2 \frac{1}{g_m^2}$$

$$= 1 + \frac{R_s}{R_g} \frac{T_g}{T} + \frac{R_{eq}}{R_s} \left( \frac{R_s + R_g}{R_g} \right)^2 \quad (39)$$

where

$\overline{i_g^2}$  = mean-squared grid noise current =  $4kBT_g/R_g$ .

$\overline{i_s^2}$  = mean-squared thermal-agitation noise current,  
 $4kTB/R_s$ , of  $R_s$ .

$\overline{i_{ns}^2}$  = mean-squared tube shot-noise current.

$\overline{i_{nr}^2}$  = mean-squared thermal-agitation noise current,  
 $4kTB/R_L$  of  $R_L$ .

$\overline{i_p^2} = \overline{i_{ns}^2} + \overline{i_{nr}^2}$  = mean-squared plate-circuit noise  
current.

$T_g$  = effective absolute temperature of the input-load-  
ing, defined as  $\overline{i_g^2} R_g / 4kTB$ .

$g_m$  = tube mutual transconductance.

$R_s$  = transformed source resistance.

$R_g$  = input resistance due to tube and coupling  
circuits.

Since it is possible to vary the source resistance by suitable impedance transforming devices, it is well to consider the value of  $R_g$  which makes the noise-figure of the

amplifying stage a minimum. Differentiating (39) shows that this is

$$R_{S_{opt}} = \sqrt{\frac{\bar{L}_p^2 R_g^2}{\bar{L}_g^2 g_m^2 R_g^2 + \bar{L}_p^2}} = \sqrt{\frac{R_g^2 R_{eq}}{R_g \left( \frac{T_g}{T} \right) + R_{eq}}} \quad (40)$$

For most cases of interest

$$\bar{i}_g^2 g_m^2 R_g^2 \gg \bar{i}_p^2 \quad (41)$$

which is equivalent to the condition

$$\frac{T_g}{T} R_g \gg R_{eq} \quad (42)$$

This permits simplifying (40) to the form

$$R_{S_{opt}} \doteq \frac{i_p}{\bar{L}_g g_m} = \sqrt{R_{eq} R_g \frac{T}{T_g}} \quad (43)$$

Equation (43) shows that the optimum source resistance is considerably lower than the value matching the input resistance of the tube; it is rather that value which makes the plate current resulting from the grid-noise voltage equal to the plate-noise current. Substituting (40) into (39) gives an expression for the optimum noise figure

$$F_{opt} = 1 + 2 \left[ \frac{R_{eq}}{R_g} + \sqrt{\left( \frac{R_{eq}}{R_g} \right)^2 + \frac{T_g}{T} \frac{R_{eq}}{R_g}} \right] \quad (44)$$

which can be simplified under the conditions of (42) to

$$F_{opt} \doteq 1 + 2 \sqrt{\frac{T_g}{T} \frac{R_{eq}}{R_g}} \quad (45)$$

or

$$F_{opt} = 1 + 2 \frac{R_{eq}}{R_{s_{opt}}} \quad (46)$$

Because  $T_g/T$  is constant for the frequency range under consideration, (45) permits one to evaluate the potential noise performance of a tube without considering circuit details, but knowing only two tube properties, namely, equivalent noise resistance and input resistance due to transit time. Equation (46) indicates the manner in which optimum noise figure increases with increasing frequency. Because

$$R_g \propto \frac{1}{f^2} \quad (47)$$

it follows that

$$R_{s_{opt}} \propto \frac{1}{f} \quad (48)$$

and hence

$$(F_{opt} - 1) \propto f \quad (49)$$

The term  $(F_{opt} - 1)$  is designated the "excess noise figure".

Experimental corroboration of (49) is shown in Fig.5, in which are shown excess noise figures measured by Wallman (21) at 6, 30, and 180 Mcs.

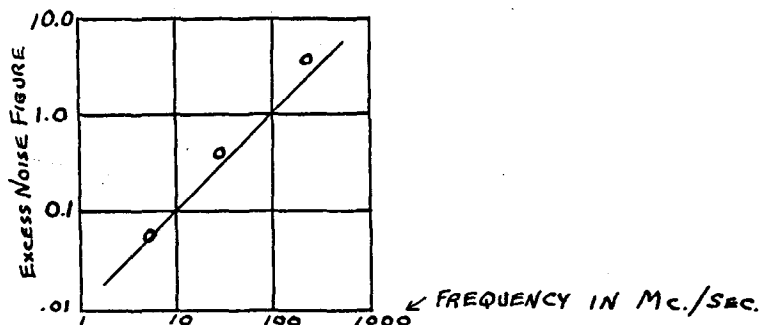


Fig.5 - Measured excess noise figures of low-noise cascode amplifiers at 6, 30, and 180 Mc.



Since the excess noise figure varies directly as the frequency, we should expect lower noise figures with lower intermediate frequencies. Such is the case if a balanced mixer is used to eliminate local-oscillator noise; 30 Mc. is the most common intermediate frequency with considerable work being done on 6 Mc. amplifiers. The lower limit of frequency is set by local-oscillator tuning, automatic frequency control, and automatic gain control considerations.

With the use of a triode connected 6AK5 grounded-cathode stage followed by a half-6J6 grounded-grid stage, the writer was able to obtain a noise figure of 1.35 at 30 Mc., which value agrees favorably with the best that can be expected of a 6AK5 stage alone. The following is a qualitative analysis of the "cascode" low noise circuit; for a precise treatment of its noise figure the reader is referred to Wallman (21).

Referring to Fig. 3, let  $g_{m1}$ ,  $r_{p1}$ ,  $g_{m2}$ , and  $r_{p2}$  be the transconductance and plate resistance of the first and second tubes, and let  $R_2$  be the load resistance of the second tube. Assuming, for simplicity, that  $R_2$  is considerably smaller than  $r_{p2}$ , as in wide band amplifiers, then one knows that the input resistance of the grounded-grid stage is approximately  $1/g_{m2}$ ; this is the resistance looking to the right at points A A' of Figure 3.

The resistance looking to the left at A A' is  $r_{p1}$ . Typical values are about 200 ohms for  $1/g_{m2}$  and 4500 ohms

for  $r_{p1}$ . It is this combination of very low resistance to the right and very high resistance to the left that is the crucial characteristic of the grounded-cathode, grounded-grid combination, with regard to both stability and noise figure.

Consider first the question of stability. The amplification from the grid of tube 1 to its plate is

$$g_{m_1} \times \frac{1}{g_{m_2}} = \frac{g_{m_1}}{g_{m_2}} \quad (50)$$

If  $g_{m1}$  and  $g_{m2}$  are about equal, the usual case, the amplification is approximately unity. This low amplification makes the grounded-cathode stage stable.

Consider next the amplification of the combination. For a 1-volt signal applied to the input grid, the plate current of tube 1 is  $g_{m1}$  ampere. Because this current flows through the plate circuit of tube 2, the voltage across  $R_2$ , and hence the amplification of the cascode, is approximately equal to  $g_{m1} \times R_2$ . With regard to amplification, the cascode is thus equivalent to a pentode of transconductance  $g_{m1}$ . It should be noted that the amplification of the cascode does not depend on  $g_{m2}$ . The motivation for large  $g_{m2}$  is essentially only this: the larger  $g_{m2}$ , the smaller is the amplification of the grounded-cathode stage, and hence the greater the stability of that stage.

The transconductance of a pentode is increased when it is connected as a triode, approximately in the ratio of cathode to plate current. For this reason, the amplification of a cascode employing a triode-connected 6AK5 as

first stage is actually about a third larger than that of a single pentode 6AK5 stage.

Consider next the noise figure. From Chapter II, the available gain of the first stage is

$$G_1 = \frac{\frac{\mathcal{U}_1^2}{4r_{p1}}}{\frac{1}{4R_s}} = \frac{\mathcal{U}_1^2 R_s}{r_{p1}} \quad (51)$$

The noise figure of the grounded-grid stage, regarding  $R_2$  as part of that stage is

$$\begin{aligned} F_2 &= 1 + \frac{\overline{i_{g2}^2}}{\overline{i_{p1}^2}} + \frac{\overline{i_{p2}^2}}{\overline{i_{p1}^2}} \left( \frac{r_{p1} + R_{g2}}{r_{p1} R_{g2}} \right)^2 \frac{1}{g_m^2} + \frac{\overline{i_{p2}^2}}{\overline{i_{p1}^2}} \\ &= 1 + \frac{\frac{4kBT_{g2}}{R_{g2}}}{\frac{4kTB}{r_{p1}}} + \frac{\frac{g_m^2 R_{g2} 4kTB}{4kTB}}{\frac{4kTB}{r_{p1}}} \left( \frac{r_{p1} + R_{g2}}{r_{p1} R_{g2}} \right) \frac{1}{g_m^2} + \frac{\frac{4kTB}{R_2}}{\frac{4kTB}{r_{p1}}} \\ F_2 - 1 &= \frac{r_{p1}}{R_{g2}} \frac{T_{g2}}{T} + \frac{R_{g2}}{r_{p1}} \frac{r_{p1} + R_{g2}}{R_{g2}} + \frac{r_{p1}}{R_2} \end{aligned} \quad (52)$$

Since  $R_{g2} \gg r_{p1}$ , this becomes

$$F_2 - 1 = \frac{r_{p1}}{R_{g2}} \frac{T_{g2}}{T} + \frac{R_{g2}}{r_{p1}} + \frac{r_{p1}}{R_2} \quad (53)$$

The first term on the right side of (53) represents grid noise; the second, plate shot noise, and the third thermal agitation noise in  $R_2$ .

For a two stage cascode, the over-all noise figure is given by

$$F_{12} = F_1 + \frac{F_2 - 1}{G_1} \quad (54)$$

Taking typical values for a 6AK5-half 6J6 cascode at 30 Mc.;

$\mu_1 = 30$ ,  $R_s = 2350$  ohms,  $T_g/T = 5$ ,  $r_{p1} = 4500$  ohms,  $R_{g2} = 60,000$  ohms,  $r_{eq2} = 500$  ohms, and  $R_2 = 2000$  ohms, we have an available gain of the first stage

$$G_1 = \frac{900 \cdot 2350}{4500} = 470 \quad (55)$$

which is extremely high, and

$$\begin{aligned} F_2 - 1 &= \frac{4500}{60,000} \cdot 5 + \frac{500}{4500} + \frac{4500}{2000} \\ &= 0.38 + 0.11 + 2.25 = 2.74 \end{aligned} \quad (56)$$

Substituting in ( 54 ) we have

$$F_{12} = F_1 + \frac{2.74}{470} = F_1 + 0.01 \quad (57)$$

In the same typical case,  $F_1$  is about 1.35. Equation ( 57 ) thus validates the assertion that the noise figure of the cascode is very nearly that of the grounded-cathode stage alone.

Consider last the available gain of the cascode, regarding  $R_2$  as part of it

$$G_{12} = \frac{\frac{(g_m R_2)^2}{4R_2}}{\frac{1}{4R_s}} = g_m^2 R_s R_2 \quad (58)$$

In the typical case under consideration,  $G_{12} \approx 200$ ; this is sufficient to make any usual third-stage noise negligible.

#### 4. Practical circuit of low noise amplifier.

The schematic of Fig. 6 shows a practical embodiment of the low noise cascode as used in the 30 Mc. i-f

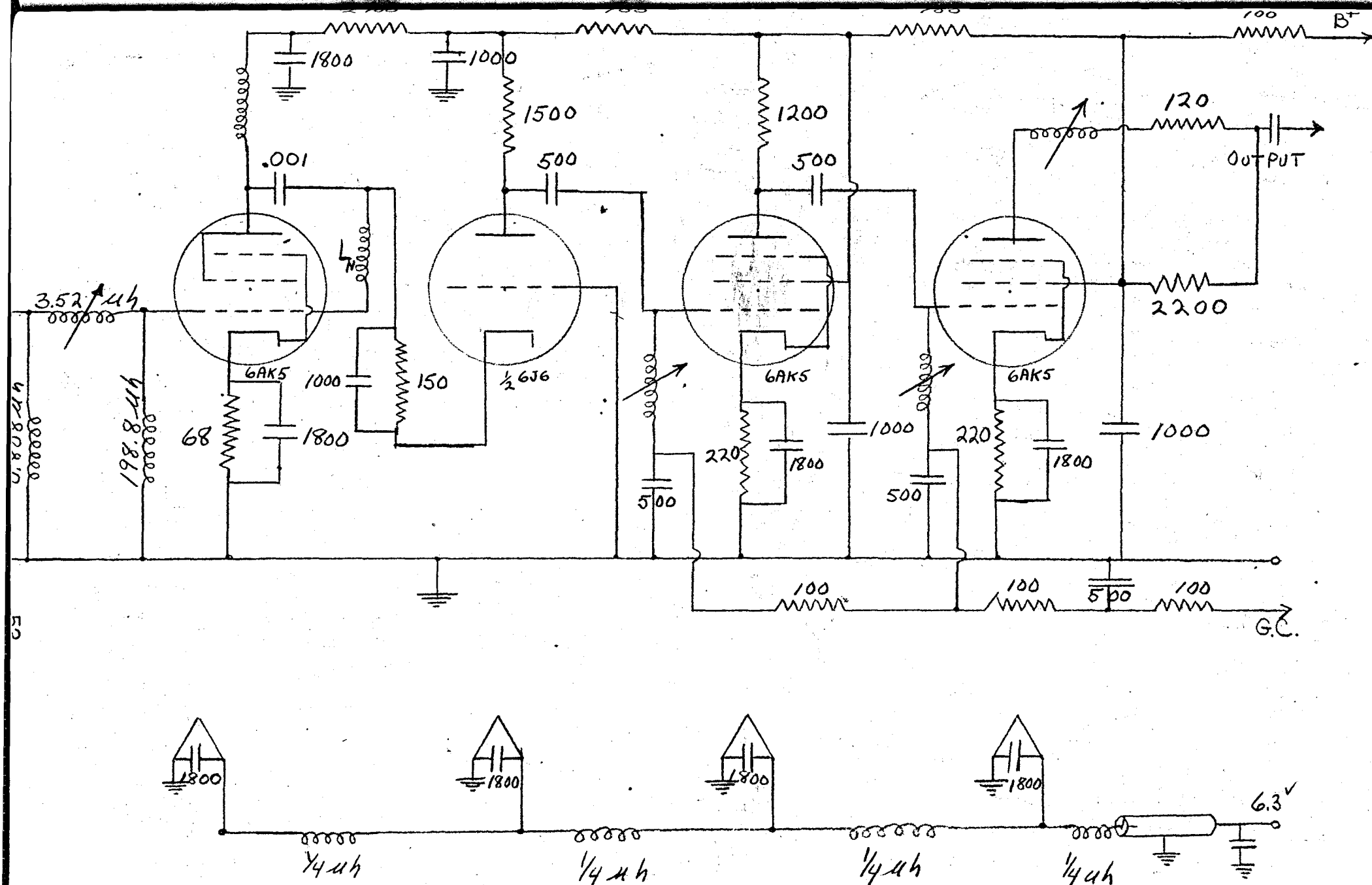
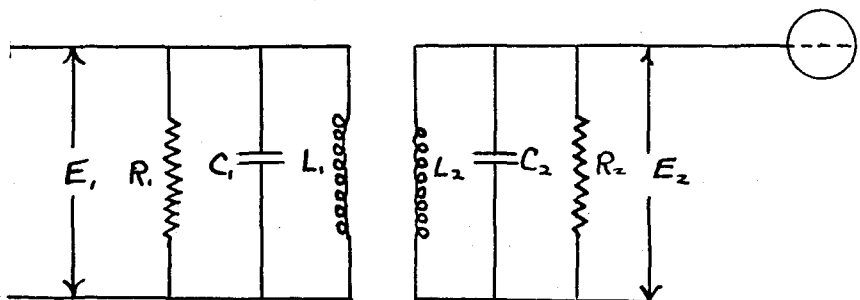


Figure 6  
Practical embodiment of the low noise cascode in a 30 Mc. i-f preamplifier

preamplifier of a radar receiver being built by the Glenn L. Martin Company. In measurements on a similar circuit the M.I.T. Radiation Laboratory obtained a mean noise figure of 1.35 as compared with 1.85 on their best amplifier using a pentode as first stage. Early measurements of the noise figure of this circuit averaged about 1.6. After various refinements had been introduced, the writer was able to obtain comparable noise figures. There follows a discussion of these refinements.

The part of the amplifier most critical from a noise standpoint is the input circuit and this circuit was the first to be investigated in an attempt to improve the amplifier noise figure. By way of obtaining the required bandwidth in the input circuit, a double-tuned inductance-coupled input network in the form of a self-inductance-coupled network was used. Of equal importance with the bandwidth is the requirement that the network present the optimum transformed source resistance to the grid of the first tube, in this case 2350 ohms for the triode-connected 6AK5. The following are the design computations for the network used and are taken from Section 5-5 of Valley (20). Curves based on the design data are shown in Fig. 7.



$$f_0 = 30 \text{ Mc.}$$

$$C_2 = 7 \text{ micromicrofarads (for neutralized 6AK5 triode,}$$

$$C_{in} = C_{gk}, \text{ since } C_{gp} \text{ is neutralized)}$$

$$Q_2 = \infty$$

$$R_1 = 200 \text{ ohms (source resistance before transformation)}$$

$$\text{Midband } R_{22} = 2350 \text{ ohms (optimum transformed source resistance for best noise figure)}$$

Curves hereinafter referred to as (a), (b), (c), (d), (e), and (f), are from Fig. 7.

$$Z_{21} = 1.42 R_1 \sqrt{\frac{C_1}{C_2}} = Z_{12} \quad \text{from curve (b)}$$

$$\text{By definition, } Z_{12} = E_2/I_1$$

Since the network is dissipationless, input and output available powers are equal:

$$I_1^2 R_1/4 = E_2^2/4R_{22}$$

$$\therefore R_{22} = 1/R_1 \times (E_2/I_1)^2 = Z_{12}^2/R_1, \text{ then } Z_{12} = \sqrt{R_1 R_{22}}$$

$$\therefore 1.42 R_1 \sqrt{C_1/C_2} = \sqrt{R_1 R_{22}}$$

$$\text{From which } C_1 = R_{22} C_2 / (1.42)^2 R_1 = \frac{2350 \times 7}{(1.42)^2 \times 200} = 40.8$$

micromicrofarads.

$$Q_1 = 2\pi f_0 R_1 C_1 = 6.28 \times 3 \times 10^7 \times 200 \times 40.8 \times 10^{-12} = 1.538$$

$$Q_1/2\pi = \frac{1.538}{2} = .245$$

Utilizing this value of  $Q_1/2\pi$  and (e), we find  $K = .428$

With this value of  $K$  established, we can find the rest of the required information; from (c)

$$f_1/f_0 = f_0/f_2' = .925$$

$$f_1 = .925 \times 30 = 27.75 \text{ Mc.}, \quad f_2' = \frac{30}{.925} = 32.4 \text{ Mc.}$$

from (d)

$$f_2/f_0 = f_0/f_1' = .975$$

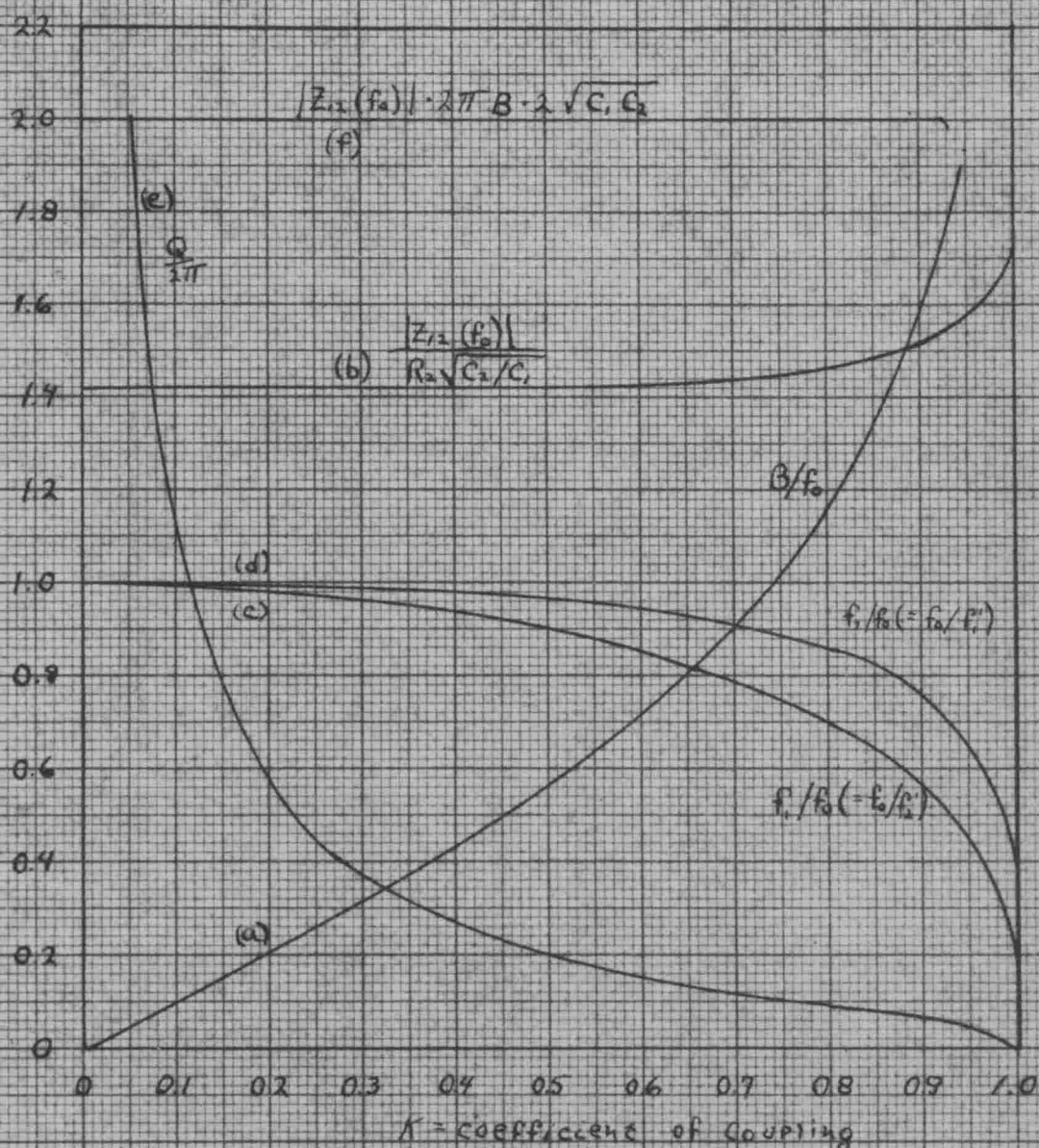


Fig.7 .- Design data for low-Q transitionally coupled double-tuned circuit,  $Q_2 = \infty$ ,  $Q_1 = Q$ . (a) Fractional bandwidth,  $B/f_0$ ; (b) normalized midband gain; (c) primary resonant frequency; (d) secondary resonant frequency; (e)  $Q/2\pi = f_0 R_1 C_1$ ; (f) gain-bandwidth factor  $|Z_{12}(f_0)| \cdot 2\pi B \cdot 2\sqrt{C_1 C_2}$



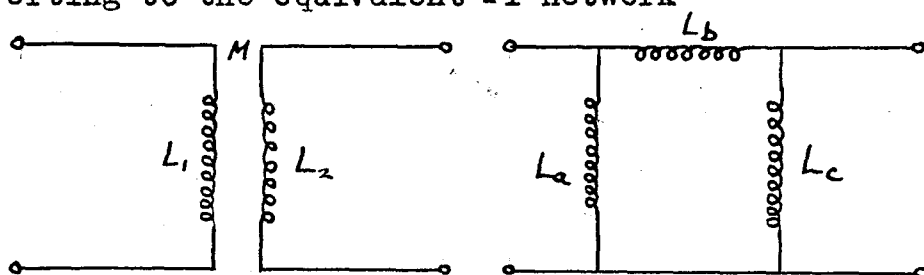
$$f_2 = .975 \times 30 = 29.25 \text{ Mc.}, f_1' = \frac{30}{.975} = 30.8 \text{ Mc.}$$

$$L_1 = \frac{1}{4\pi^2 f_1^2 C_1} = \frac{1}{4\pi^2 (27.75)^2 10^{-12} \times 40.8 \times 10^{-12}} = .805 \mu\text{h}$$

$$L_2 = \frac{1}{4\pi^2 f_2^2 C_2} = \frac{1}{4\pi^2 (29.25)^2 10^{-12} \times 7 \times 10^{-12}} = 4.235 \mu\text{h}$$

$$M = K\sqrt{L_1 L_2} = .428 \sqrt{.805 \times 4.235} = .791 \mu\text{h}$$

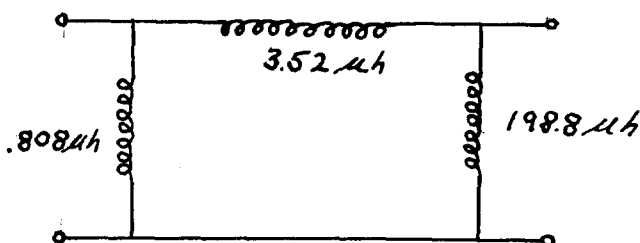
Converting to the equivalent Pi network



$$L_a = \frac{L_1 L_2 - M^2}{L_2 - M} = \frac{3.41 - .63}{3.444} = .808 \text{ microhenry}$$

$$L_b = \frac{L_1 L_2 - M^2}{M} = \frac{2.78}{.791} = 3.52 \text{ microhenrys}$$

$$L_c = \frac{L_1 L_2 - M^2}{L_1 - M} = \frac{2.78}{.014} = 198.8 \text{ microhenrys}$$



from (f)

$$Z_{12} \times 2\pi \times B \times 2\sqrt{C_1 C_2} = 2$$

$$B = \frac{1}{2\pi Z_{12} \sqrt{C_1 C_2}} = \frac{1}{2\pi \sqrt{R_1 R_2} C_1 C_2}$$

$$\begin{aligned}
&= \frac{1}{2\pi Z_{12} \sqrt{200 \times 2350 \times 40.8 \times 7 \times 10^{-24}}} &= \frac{1}{2\pi \sqrt{134.4 \times 10^{-9}}} \\
&= \frac{1}{2\pi \times 11.59 \times 10^{-9}} &= 13.73 \text{ Mc.}
\end{aligned}$$

The above input network was built with  $L_c$  omitted and  $L_a$  made a bifilar winding (for use with a balanced mixer). Maximum gain occurred at 31.9 Mc.. Half-power points were at 26.7 and 36.8 Mc., giving a bandwidth of 10.1 Mc.. The reduction in bandwidth from that computed might have been caused by imperfect neutralization of the input tube off band center, resulting in a change in input capacity which is positive above band center and negative below.

The input circuit for which the component values were computed above, was substituted for the original input circuit with a resultant reduction in noise figure from about 1.6 to 1.35. As mentioned above, this noise figure approximates very well the best noise figure previously obtained with such a circuit.

## 5. Neutralization considerations

It is pointed out in Wallman (21) that neutralization of the grid to plate capacitance has an important effect on noise figure. In his original circuit, Wallman uses "coil neutralization" in which the neutralizing inductance  $L_n$  is resonated with the grid-plate capacitance  $C_{gp}$  at the mid-band frequency, in our case 30mc. The schematic of this system is shown below.

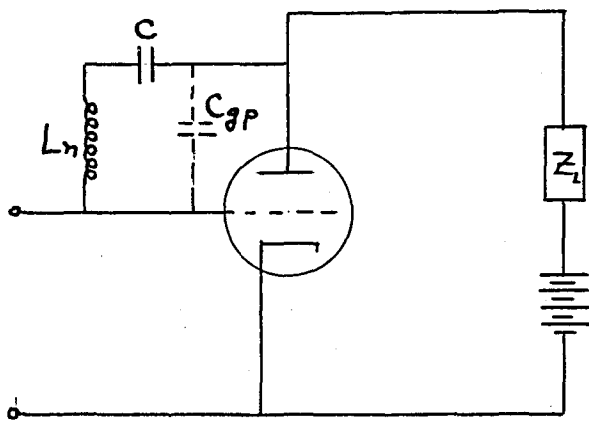


Figure 8  
Coil neutralization of grid-plate capacitance

This arrangement is effective at only one frequency and is very critical of adjustment. It is necessary that the  $Q$  of the neutralizing coil be high if the resonant impedance is to be large. This means a relatively large coil form and prohibits the use of a variable inductance (slug tuned). The correct adjustment of  $L_n$  is very difficult to accomplish. It was noted that the location of  $L_n$  with respect to the coils of the input circuit had a marked effect on the frequency at which neutralization occurred. It was found necessary to locate  $L_n$  so as to allow minimum coupling with other inductances and to replace it when necessary in the same relative position.

Since the above form of neutralization is so difficult to adjust and is, moreover, effective at only one frequency, it was decided to try the neutrodyne (Hazeltine) system of neutralization as shown in the schematic below.

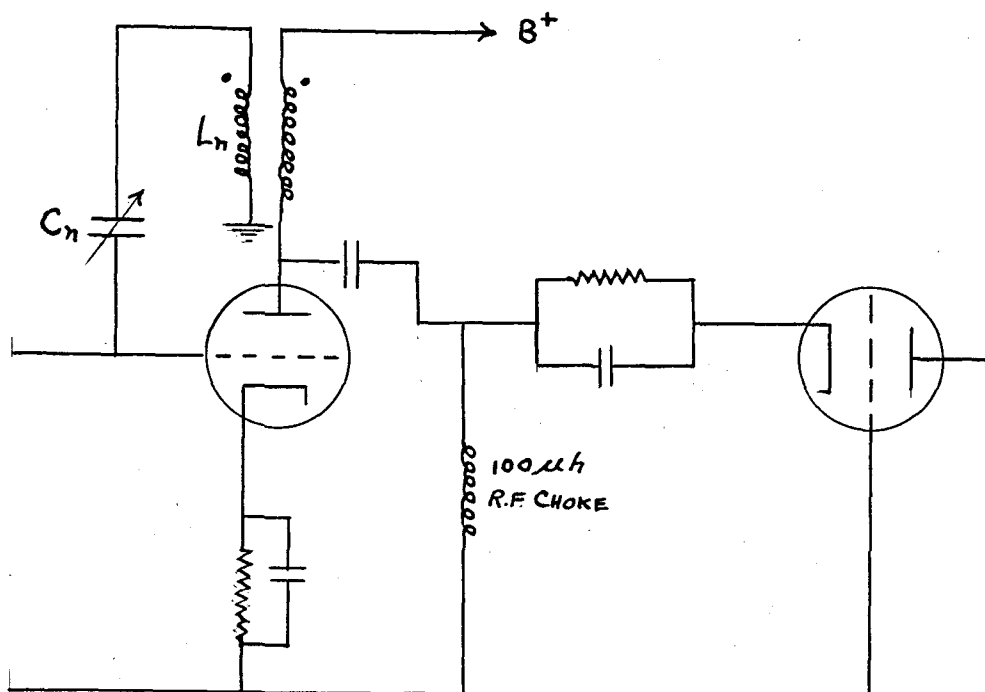


Figure 9

Neutrodyne (Hazel tine) neutralization of  $C_{gp}$ .

This system of neutralization has several advantages, namely (1) relatively independent of frequency, and (2) easily adjusted by the use of a small variable condenser included as  $C_n$ . It is obvious that with this form of neutralization, the input capacitance is no longer simply  $C_{gp}$  as it is in the case of coil neutralization. Instead it is, for perfect neutralization, the sum of  $C_{gk}$ ,  $C_{gp}$ , and  $C_n$ . It is to be expected, therefore, that the new form of neutralization will require a new input circuit if the tube is to see the desired optimum transformed source resistance. Conversely, if the old input network is used with the new system of neutralization, the resistance presented to the tube is incorrect and the noise figure can be expected to deteriorate. Such is found to be the case and the noise figure is actually greater than 2 as compared

with the 1.35 obtained with coil neutralization and the same input network.

A new input circuit was designed for the amplifier with Hazeltine neutralization, by the method of Section 4. This design called for  $L_a = .538$  microhenry,  $L_b = 3.55$  microhenrys, and  $L_c = 16.9$  microhenrys. This input circuit was built and tested in the amplifier and with it we were unable to obtain a noise figure better than 1.5. Time did not permit further investigation of the circuit by the writer and the problem was given to a Martin engineer for further investigation.

In his article on a low-noise amplifier, Wallman (21) recognizes the cost of the improvement in noise figure as being one extra tube, and at the same time mentions the possibility of using the then new 2C51 double triode to yield the advantages of this circuit with a single envelope. With this in mind, the writer undertook to build and test a circuit, the schematic of which is shown in Fig. 10, employing the 2C51 in this manner. The results were most gratifying, the modified amplifier producing noise figures as good as any obtained with the original 6AK5-half 6J6 combination.

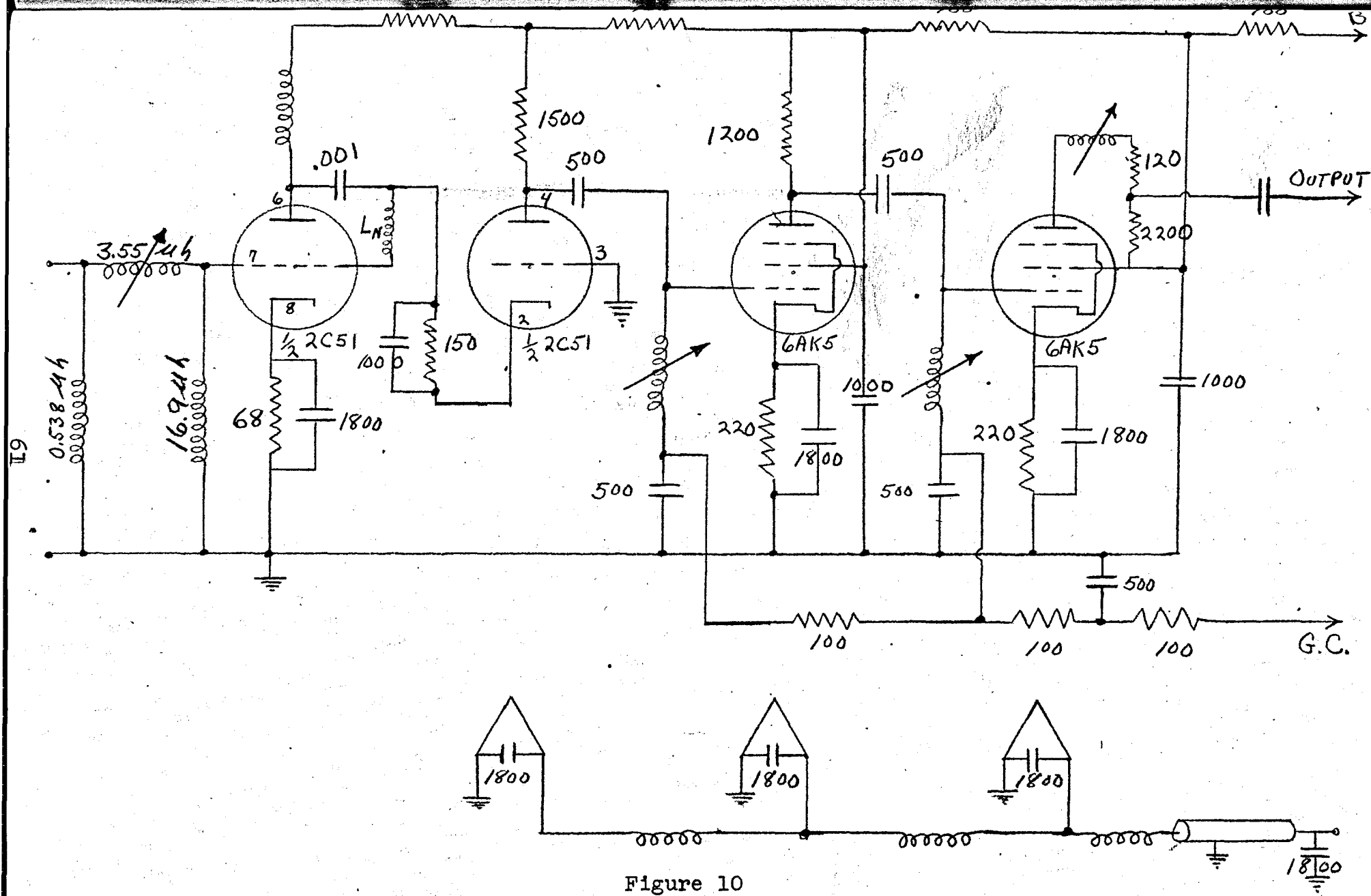


Figure 10

Low noise cascode employing a single 2 C 51 tube in a 30 Mc. preamplifier

## CHAPTER V

### MEASUREMENT OF NOISE FIGURE

#### 1. Method of measuring noise figure

The measurement of noise figure affords an effective method of checking the ability of an amplifier to detect weak signals. In all work on noise figure by the writer, measurements were made with a noise generator of the type shown in Fig. 11. The outstanding feature of noise generators is that their available power is proportional to an easily measured direct current. In the case of the temperature-limited diode, the constant of proportionality between the available power and the direct current is easily calculated and it can be used as an absolute instrument up to about 300 Mc./sec.

A temperature-limited diode acts like a generator of noise current having a certain root-mean-square value  $I_n$ , because of the shot effect. The mean-squared current,  $\overline{I_n^2}$ , is given by

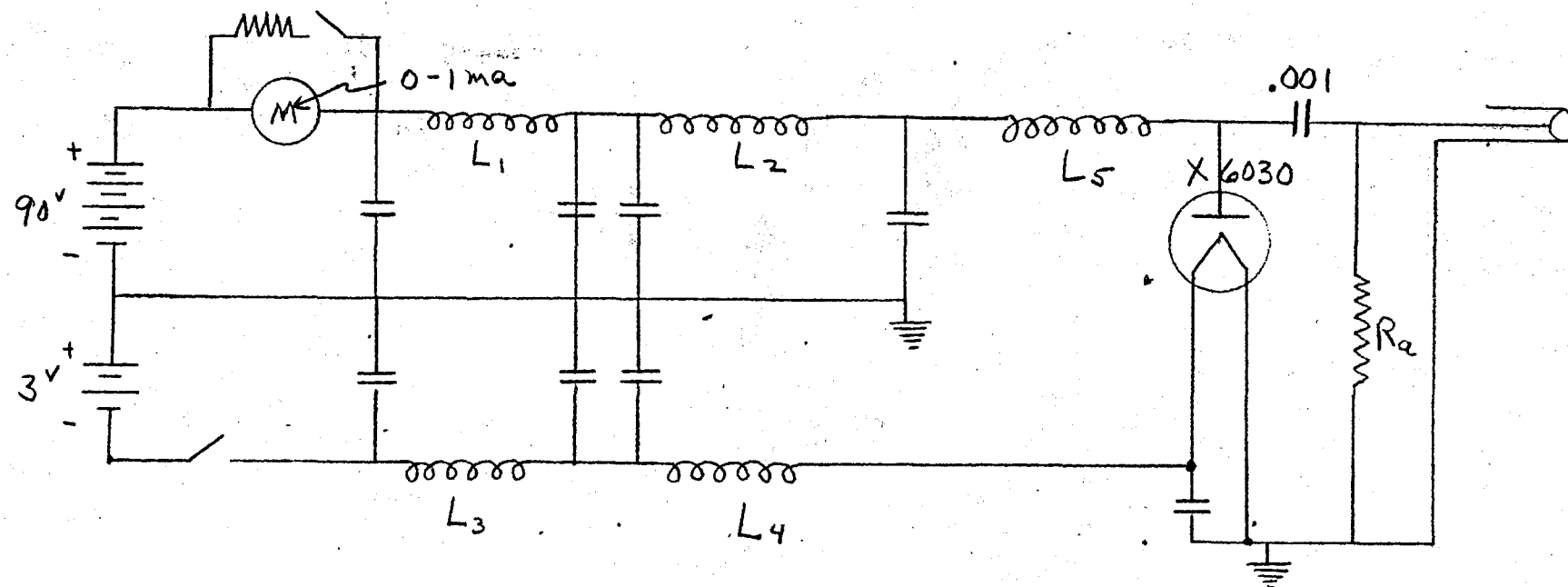
$$\overline{I_n^2} = 2eIB, \text{ where} \quad (59)$$

$e$  = charge of the electron =  $1.6 \times 10^{-19}$  coulomb

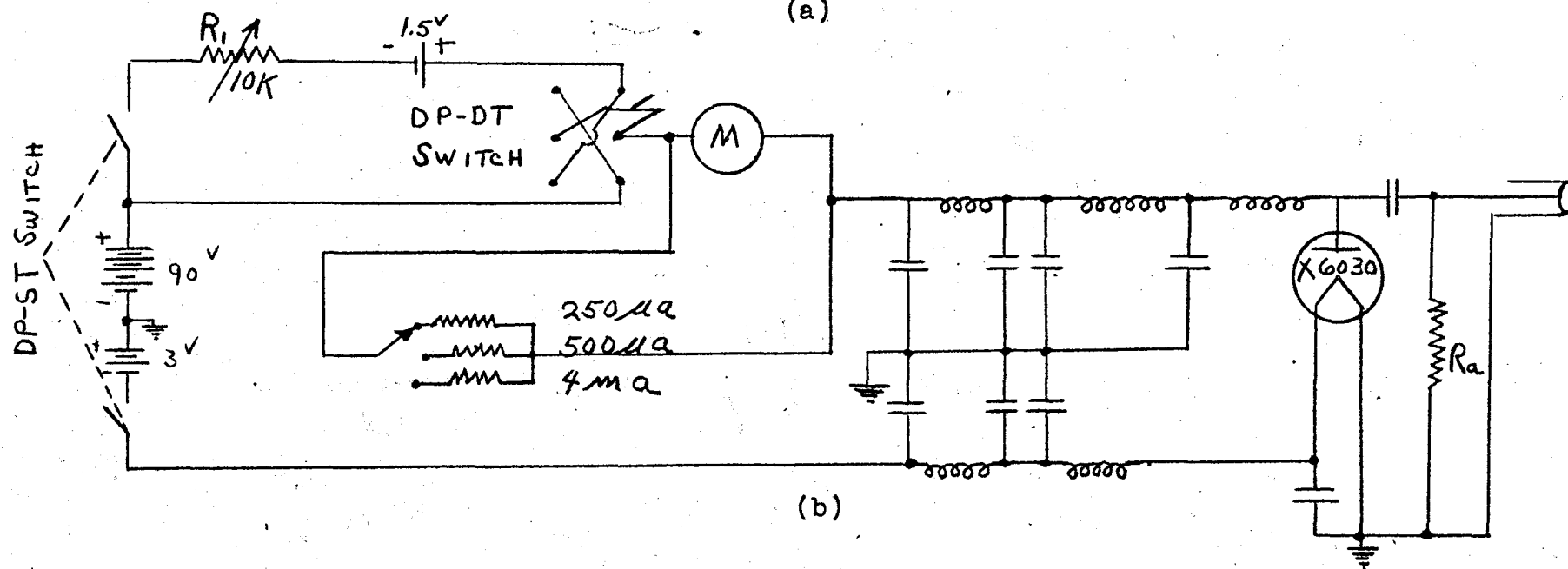
$I$  = direct current through the diode in amperes

$B$  = bandwidth of the device being used to observe the noise.

A simple noise generator consists of such a diode connected in parallel with a resistance  $R_a$  equal to the resistance of the signal source impedance and a reactance simulating the parallel reactance of the signal source. This combination is connected to the input of the amplifier



(a)



(b)

Figure 11

Schematic of typical noise generator circuit



and the value of  $I$  is adjusted by varying the diode filament current to double the noise output of the amplifier.

The noise figure is measured by first observing the indication of the output meter with the diode filament unenergized. Under these conditions the noise output is the equivalent of that produced by the network and source. Unless the meter matches the network, it will not read the available output noise power but a quantity proportional to it. Let  $p$  be the constant of proportionality. The meter then reads

$$N_p = FGkTBp \quad (60)$$

The diode is now energized and the cathode current is adjusted so as to double the output power. For this condition, the diode noise current contributes a noise voltage which produces the same output noise power as the source in the network and  $R_s$ .

Now consider the available power due to the diode and  $R_a$  considered as a signal generator. A constant current source feeding a resistance  $R_a$  is equivalent to a constant voltage generator of the same internal impedance and an open circuit voltage  $I_n R_a$ . The available power from such a generator is  $I_n^2 R_a / 4$ . The available output noise power due to the diode must, therefore, be  $GI_n^2 R_a / 4$ . For the condition when the output has been doubled, it follows that

$$\frac{GI_n^2 R_a}{4} \times p = N_p = FGkTBp \quad \text{or} \quad (61)$$

$$\frac{3.18 \times 10^{-19} \text{ IBR}_a}{4} = FkTB \quad \text{or}$$

$$F = \frac{3.18 \times 10^{-19} \text{ IR}_a}{4kT} \quad (62)$$

The beauty of the result and method is that the bandwidth does not appear in the expression. This does not, of course, mean that the noise figure is independent of bandwidth; it simply indicates that in this method of measurement, the bandwidth does not appear.

If one chooses 288° K for T, expresses I in milliamperes, and R<sub>a</sub> in ohms

$$F = 2 \times 10^{-2} \text{ IR}_a \quad (63)$$

If the source is 50 ohms, as it is in many applications, one has

$$F = I \quad (I \text{ in m.a.}) \quad (64)$$

This simple result is obtained, as was pointed out in Chapter II, by adopting 288° K as the reference temperature. It does not hold for any other temperature.

It will be recalled from preceding paragraphs that the technique of noise figure measurement requires the doubling of the output power. Experience of others, the Radiation Laboratory in particular, has indicated that most difficulties encountered in noise figure measurements are caused by improper methods of measuring relative power output of the amplifier.

The method shown in block form in Fig. 12(b) is considered the most accurate and generally satisfactory means of

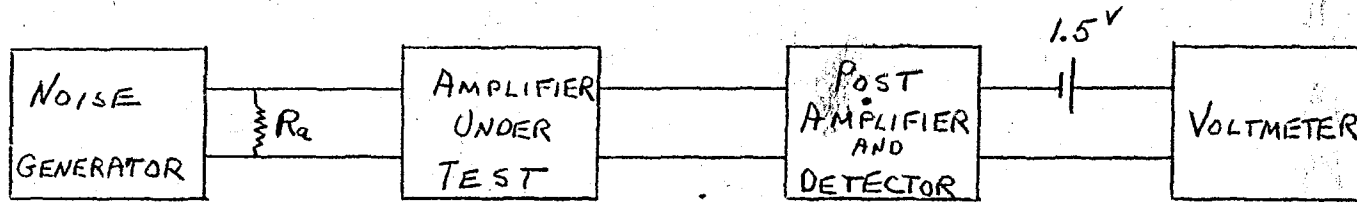


FIG. 12(a)

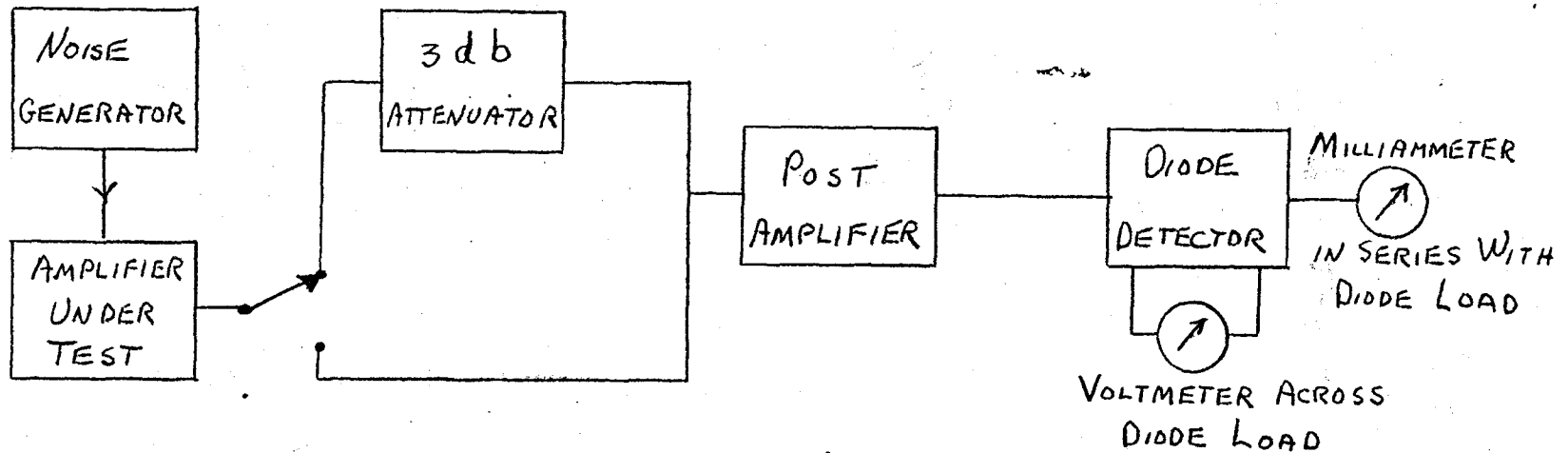


FIG. 12(b)

Block diagram of layout used in noise figure measurements

comparing amplifier output powers. This method is also used in Fig. 12(a) with the attenuator built into the postamplifier. The procedure is as follows

1. Observe reading of output meter with attenuator switched out and the noise generator off.
2. Switch attenuator in and adjust noise generator to give same meter deflection as before.
3. Since the power ratio,  $\alpha$ , of the attenuator is equal to two (2), the available power of the noise generator must have been that required to double the amplifier output power.

In noise figure measurements on low noise amplifiers such as that described in Chapter IV, certain refinements in technique may be found useful in improving the accuracy. Certain of these are concerned with the design of a noise generator, which will be covered in Section 2 of the present chapter. Another involves the use of a direct-current bucking voltage in the output of the postamplifier to permit the use of the most sensitive scale on the output meter.

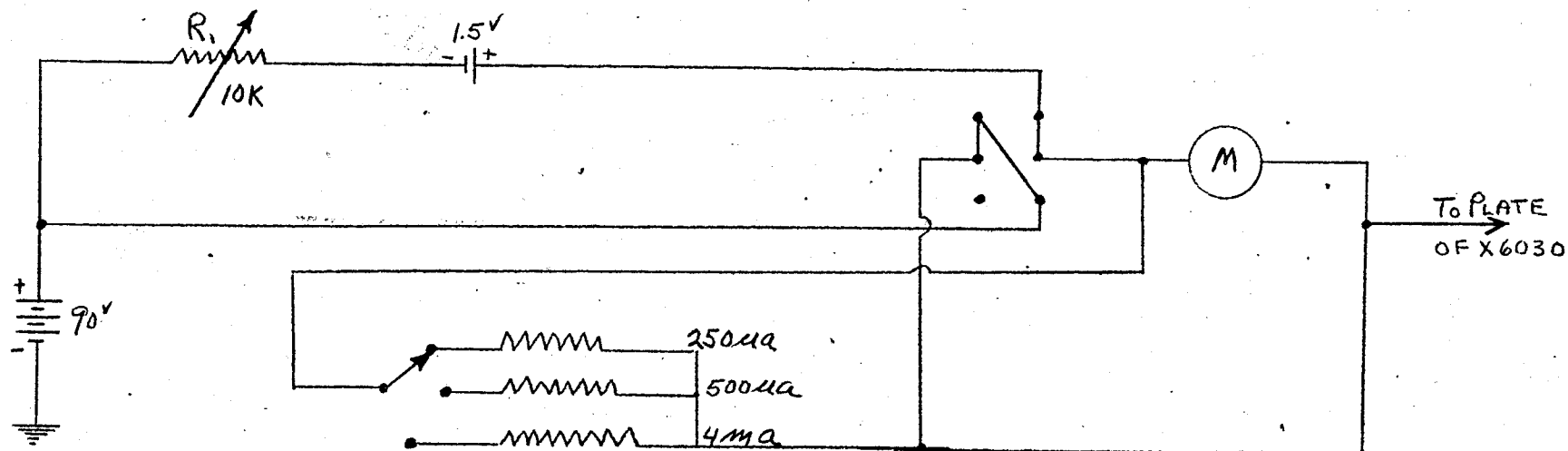
In the case of measurements made by the writer, a 1.5 volt dry battery was employed to permit the use of the 1 volt scale on the Hewlett-Packard 410-A vacuum-tube-voltmeter.

## 2. Design of a noise generator

The noise generator as originally designed is shown in schematic form in Fig. 11(a). The Sylvania X6030 diode is used in lieu of a British tube, the CV172, since the latter is not generally available. Coils  $L_1$ ,  $L_2$ ,  $L_3$ , and  $L_4$  are wound with #26 enamel wire on 2WIRC 0.25M; self

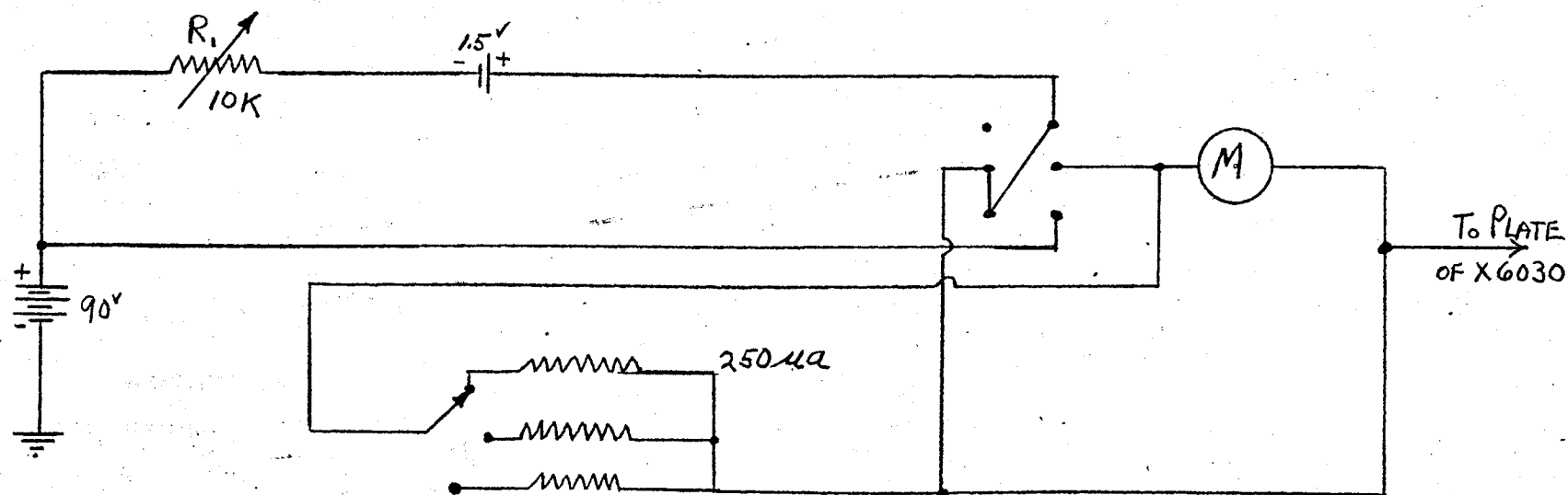
resonant at 30Mc.  $L_5$  is wound with #26 enamel wire on Speer form and tunes to 30 Mc. with capacitance from plate to ground. Condensers are 500 micro-micro-farad Erie buttons.

This circuit proved satisfactory for approximate noise figure measurements but, with a 0-1 milliamperemeter in the plate circuit, did not provide the accuracy desired in the determination of small noise figures with which we were working, i.e.  $1 < F \leq 2$ . It was then decided to substitute a 250 micro-ampere meter and to buck out the excess current with a suitably placed 1.5 volt battery. The product of this decision is the arrangement shown in Fig. 11(b), employing a double-pole-double-throw switch to give either the balancing current alone or the algebraic sum of the diode and balancing currents. It can be seen from equation ( 63 ) that a current of 250 micro-amperes with a source resistance of 200 ohms corresponds to a noise figure of 1. Hence, with the switch in the balance position, Fig.13(a),  $R_1$  is varied to obtain full-scale deflection. Now with the switch in the current sum position of Fig. 13(b), zero deflection of the meter will indicate a noise figure of 1, full scale a noise figure of 2. All of the above presupposes a source resistance of 200 ohms, which is the one most frequently used in this report. If some other value of source resistance is to be used, the actual current reading of the meter plus 250 microamperes can be substituted into equation ( 63 ) to compute the noise figure. In the actual construction of the noise generator, we were forced to use a 200 micro-ampere meter, appropriately



BALANCE CURRENT - SWITCH UP

(a)



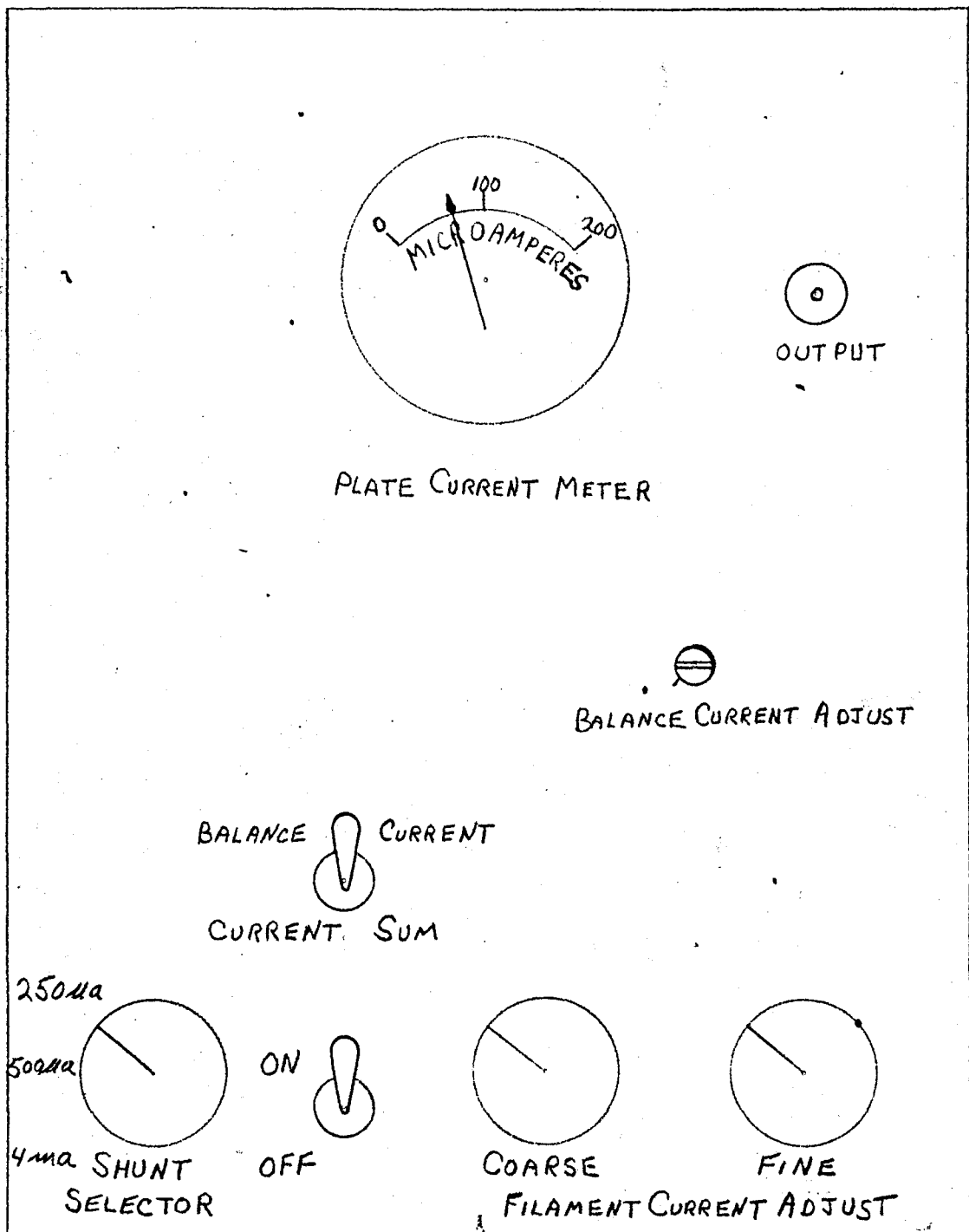
(b)

CURRENT SUM - SWITCH DOWN

Figure 13  
Noise generator switching circuit

shunted to 250 micro-amperes, 500 micro-amperes, and 4 milliamperes full-scale deflection for various positions of the meter shunting switch.

The use of such a sensitive meter as that described above requires the use of a continuously variable resistance potentiometer in the filament supply in order to obtain very small changes in the diode plate current. The conventional wire-wound potentiometer with the resistance changing in finite steps was found to be unsatisfactory and a substitute was sought. A small Helipot was felt to be the ultimate solution but, since none was available on short notice, an interim substitute was made and used. This substitute took the form of a single piece of nichrome resistance wire, placed along the top edge of the potentiometer and shorting its turns. This provided a continuously variable resistance from 0 - 0.3 ohms and, when used in conjunction with the coarse filament control, permitted very accurate settings of the diode plate current. The various controls are shown in Fig. 14.



# NOISE GENERATOR

Figure 14

Noise generator control panel



## BIBLIOGRAPHY

1. Bell, D.A. A theory of fluctuation noise. Journal of the Institution of Electrical Engineers. 82:522-536, 1938.
2. Burgess, R.E. Noise in receiving aerial systems. Proceedings of the Physical Society of London. 53, part 3:293-303, 1941.
3. Dicke, R.H. The measurement of thermal radiation at microwave frequencies. Radiation Laboratory Report #787, August 22, 1945.
4. Friis, H.T. Noise figures of radio receivers. Proceedings of the Institute of Radio Engineers. 32:419-422, July, 1944.
5. Goldberg, H. Some notes on noise figures. Proceedings of the Institute of Radio Engineers. 36:1205-1214, October, 1948.
6. Johnson, J.B. The Schottky effect in low frequency circuits. Physical Review. 26:71-85, 1925.
7. Johnson, J.B. Thermal agitation in conductors. Nature. 119:50, 1927.
8. Johnson, J.B. Thermal agitation of electricity in conductors. Physical Review. 29:367-368, 1927.
9. Johnson, J.B. Thermal agitation of electricity in conductors. Physical Review. 32:97-113, 1928.
10. Johnson, J.B., and F.B.Llewellyn. Limits to amplification. Electrical Engineering. 53:1449-1453, November, 1934.
11. Llewellyn, F.B. A study of noise in vacuum tubes and attached circuits. Proceedings of the Institute of Radio Engineers. 18:243, February, 1930.
12. Moullin, E.B., and C.D.Ellis. The spontaneous background noise in amplifiers due to thermal agitation and shot effects. Journal of the Institution of Electrical Engineers. 74:323-345, 1934.
13. North, D.O., and W. R. Ferris. Fluctuations induced in vacuum tube grids at high frequencies. Proceedings of the Institute of Radio Engineers. 29:49-50, February, 1941.

14. North, D.O. Absolute Sensitivity of radio receivers. R.C.A. Review. 6:332-343, January, 1942.
15. Nyquist, H. Thermal agitation of electric charge in conductors. Physical Review. 32:110-113, 1928.
16. Pound, R.V. Microwave mixers. New York, McGraw-Hill. 1948. (Massachusetts Institute of Technology. Radiation laboratory series. No. 16)
17. Sandeman, E.K., and L.H. The E.M.F. of thermal agitation. Philosophical Magazine. 7:774-782, 1929.
18. Schottky, W. On spontaneous current fluctuations in various electric conductors. Annalen der Physik. 57:541-567, 1918.
19. Thompson, B.J., D.O. North, and W.A. Harris, Fluctuations in space charge limited diodes at moderately high frequencies. R.C.A. Review. V 4 and 5. January 1940 to July, 1941. A series of five papers.
20. Valley, G.E. Jr. Vacuum tube amplifiers. New York, McGraw-Hill. 1948. (Massachusetts Institute of Technology. Radiation laboratory series. No.18)
21. Wallman, H., A.B. MacNee, and C.P. Gadsden. A low-noise amplifier. Proceedings of the Institute of Radio Engineers. 36:700-708, June, 1948.
22. Williams, F.C. Fluctuation noise in vacuum tubes which are not temperature-limited. Journal of the Institution of Electrical Engineers. 78:326-332, 1936.
23. Ziegler, M. Causes of noise in amplifiers. Philips Technical Review. 2:136-141, May, 1937.